Ricardo Luís Baptista Agostinho

BodyEnergyExpenditure: Automatic Measurement of Energy Expenditure Associated to Physical Exercise

Master's dissertation submitted to the Department of Electrical and Computer Engineering of
Faculty of Science and Technology of the University of Coimbra,
in partial fulfillment of the requirements for the Degree of Master in Electrical and Computer Engineering,
specialization in Computers
October 2020

· U C ·

Universidade de Coimbra

BodyEnergyExpenditure: Automatic Measurement of Energy Expenditure Associated to Physical Exercise

Ricardo Luís Baptista Agostinho

Supervisors

Prof. Rui P. Rocha, PhD

Prof. Paulo Menezes, PhD

Jury

Prof. Manuel M. Crisóstomo, PhD

Prof. Luís M. Rama, PhD

Prof. Rui P. Rocha, PhD

Master's dissertation submitted to the Department of Electrical and Computer Engineering of Faculty of Science and technology of the University of Coimbra, in partial fulfillment of the requirements for the Degree of Master in Electrical and Computer Engineering, specialization in Computers.

October 2020

Interreg
España - Portugal

Fondo Europeo de Desarrollo Regional
Fundo Europeu de Desenvolvimento Regional

Cofinanciado por:

This dissertation project was supported by the EuroAGE project, which is funded by Interreg V A Spain - Portugal program under Grant No. POCTEP-0043_EUROAGE_4_E. It was also supported by the Institute of Systems and Robotics (ISR) – University of Coimbra, funded by "Fundação para a Ciência e a Tecnologia" (FCT) under Grant No. UID/EEA/00048/2019.

Acknowledgments

To my supervisors, professor Rui P. Rocha and professor Paulo Menezes for providing me the opportunity to work in this dissertation. To professor Luis Rama for the help, dedication and knowledge provided during this dissertation. To the EuroAGE project with ref. POCTEP-0043_EUROAGE_4_E, funded by the Interreg Spain-Portugal program, which financed the hardware acquisition needed for the development of this dissertation. To the Institute of Systems and Robotics for providing the logistical conditions for the development of the work, namely the job position in the laboratory and the test room for carrying out the experiments. To professor Paulo Coimbra, who loaned the treadmill to carry out the experiments. To my colleagues from MRL and IS3L for your collaboration in this work. To my swimming colleagues and coaches, for your collaboration and friendship over these years. To my grandparents, with a special thanks to my grandmother São for the help and affection you give me that every grandson needs. And my biggest thanks to my parents and brother Miguel for all the support you have given me over the years. Without you, none of this would have been possible.

Coimbra, October 2020

Resumo

A medição do dispêndio energético associado ao exercício físico é relevante em vários domínios. No desporto de alto rendimento, permite monitorizar as necessidades energéticas de cada atleta e gerir o seu esforço físico durante o treino, ajudando na prevenção de lesões e na obtenção de melhores resultados desportivos. No contexto clínico, pode ajudar na prevenção do aparecimento de diversas doenças crónicas, tais como diabetes, obesidade e doenças cardiovasculares.

Os métodos de estimação de dispêndio energético usados em laboratório são os mais bem aceites pela comunidade científica. No entanto, devido ao seu custo, necessidade de pessoal qualificado e restrição a ambiente de laboratório, tornam-se pouco práticos. Alternativas como o uso de acelerómetros ou de cardiofrequencímetros têm maior interesse prático, por serem mais baratos, menos intrusivos e fornecerem informação em tempo real. Além disso, este tipo de abordagem pode ser usada em qualquer lugar, durante a realização de qualquer tipo de exercício físico.

Tendo por base o estudo prévio dos métodos de estimação do dispêndio energético do corpo humano, pretende-se com esta dissertação de mestrado desenvolver e validar um protótipo de um medidor vestível de dispêndio energético associado ao exercício físico, baseado na utilização de diferentes sensores de baixo custo e em métodos de fusão sensorial. Para efeitos de validação, foram considerados três tipos de exercício físico: corrida, ciclismo *indoor* e CrossFit. Consoante o tipo de exercício, são escolhidos o tipo e número de sensores adequados, assim como a sua colocação no corpo. Os sinais produzidos pelos sensores são posteriormente processados e integrados em modelos matemáticos desenvolvidos para a estimação de dispêndio energético. Os resultados das experiências realizadas demonstram que a solução desenvolvida pode ser considerada uma alternativa mais barata e menos intrusiva comparativamente aos métodos de referência usados em laboratório.

Palavras-Chave: Dispêndio energético, exercício físico, medidor automático, sensores, fusão sensorial

Abstract

The measurement of energy expenditure associated to physical exercise plays an important role in multiple fields. It can be used to help monitor energy requirements in athletes, in order to manage their physical effort, maintain energy balance during training and prevent injuries. It is also used for epidemiological studies and is extremely important in the global context of non-communicable diseases, such as diabetes, obesity, and cardiovascular diseases.

The most widely accepted methods by the scientific community restrict data collection to controlled settings. Despite delivering the most accurate results, they are expensive, require qualified personnel and cannot be executed outside the laboratory environment. Alternative approaches, such as the use of accelerometers, heart rate monitors or armbands, are more practical, more economical, easy to use, and less intrusive, providing real-time information. Furthermore, they can be used anywhere while performing any type of workout.

Based on the review of the different methods used to estimate energy expenditure associated to physical exercise, the main goal of this dissertation is to develop and validate a prototype for a low cost, non-intrusive wearable energy meter, based on the use of different sensors and sensor fusion methods. For validation purposes, three types of physical exercise were considered: running, indoor cycling and CrossFit. Depending on the type of exercise selected, the type and number of appropriate sensors are chosen, as well as their placement on the body. The sensor signals are subsequently processed and integrated into developed mathematical models for the estimation of energy expenditure. The results of the experiments carried out demonstrate that the developed prototype can be considered a cheaper and less intrusive solution compared to the reference methods used in the laboratory.

Keywords: Energy expenditure, physical exercise, energy meter, sensors, sensor fusion

Contents

Acronyms

SmO_2 Muscle Oxygen Saturation. xviii, xxi, 16, 17, 38, 39, 42, 50

SpO_2 Peripheral Capillary Oxygen Saturation. 16, 17

ACSM American College of Sports Medicine. 20

AEE Activity Energy Expenditure. 13

API Application Programming Interface. 53

BLE Bluetooth Low Energy. 45, 48, 49, 54

BMX Bicycle Motocross. 20

bpm beats per minute. 7, 8, 15, 22, 35

BT Bluetooth. xviii, 32, 46, 47

CE Caloric Expenditure. 7

CI Confidence Interval. xxi, 42, 50, 53

CSV Comma Separated Value. 54, 55

DC Direct Current. 36

DLW Doubly Labeled Water. 1, 2

EDA Electrodermal Activity. xvii, xviii, xxi, 17, 18, 25, 26, 28, 30, 35, 36, 39, 41, 42, 46, 47, 54, 55

EE Energy Expenditure. xviii, xxi, 1–6, 8, 9, 13–15, 21, 30, 41, 42

EMG Electromyography. 16, 17, 24, 27

ExEE Exercise Energy Expenditure. 13

FCDEF-UC Faculdade de Ciências do Desporto e Educação Física - Universidade de Coimbra. 9, 24, 28, 35, 43, 49, 57

GATT Generic Attribute Profile. 49

HIIT High-intensity Interval Training. 7

HR Heart Rate. 15, 42, 86

HW Hardware. 55

I2C Inter-Integrated Circuit. 47, 48

ICC Intraclass Correlation. xxi, 50, 53

IDE Integrated Development Environment. 54

MAE Mean Absolute Error. 30, 41

MEMS Microelectromechanical Systems. 32, 47, 54, 55

MET Metabolic Equivalent. 8, 11, 12

MHR Maximum Heart Rate. 7, 15

NEAT Non-exercise Activity Thermogenesis. 13

PA Physical Activity. 1–5, 14, 15

PAI Physical Activity Intensity. 7

PC Personal Computer. 54–56

PCB Printed Circuit Board. xviii, 46–48, 51–54, 56, 67–69

REE Resting Energy Expenditure. 12, 13

RFCOMM Radio Frequency Communication. 45, 48, 54

RMSE Root Mean Square Error. 30, 41, 55

SIG Bluetooth Special Interest Group. 49

SW Software. 55

TEE Total Energy Expenditure. 12, 13

TEF Thermic Effect of Feeding. 12, 13

THR Training Heart Rate. 7

UTCI Universal Thermal Climate Index. 71

UUID Universal Unique Identifier. 49

List of Figures

List of Tables

1 Introduction

Physical activity (PA) assessment approaches are commonly used to estimate energy expenditure (EE) in various situations. They can be used to help to monitor energy requirements in athletes, manage their physical effort, maintain energy balance during training, and prevent injuries. They are also used for epidemiological studies and are extremely important in the global context of non-communicable diseases, such as cancer, diabetes, or pulmonary and cardiovascular diseases, allowing the estimation of nutrient requirements for patients during nutrition support [38]. The prediction of energy metabolic costs can also assist wearable robotic devices (e.g. powered prostheses and exoskeletons) designed to aid people who suffer from disabling conditions, such as stroke, amputation or other mobility problems [6].

EE is difficult to measure as it depends on several factors, such as the individual's physical and metabolic characteristics, the type of PA involved, or the context in which the activity is performed. The most widely accepted methods by the scientific community are those that measure EE directly. Among them is the Doubly Labeled Water (DLW) method [20] that accurately measures the average metabolic rate over a period of time in a non-intrusive way, allowing the subjects to execute their normally daily activities. On the other hand, this is a high-cost method that requires qualified personnel and sample collection, which requires a long period between samples collection and results output. Alternative approaches estimate energy costs indirectly by measuring physiological variables correlated with EE (e.g., heart rate, body parts acceleration, oxygen saturation)[38]. These methods are more practical as they are more economical, easy to use, less intrusive, providing information in real-time. Furthermore, they can be used anywhere, while performing any type of workout. The drawback of these indirect methods is that they require mathematical models and calibrations customized to the individual's specific characteristics, type of activity, device placement and sensitivity, which can challenge the delivery of accurate results.

To choose the most appropriate method for EE estimation, one must carefully analyze each approach's strengths and limitations, as well as the context in which the physical

exercise is performed. It is the aim of this work to perform such analysis, in order to develop and validate a prototype for a low-cost wearable energy meter of the human body, based on the use of multiple sensors and sensor fusion methods. The next section reviews some assessment methods for EE estimation, as well as devices used and mathematical models for the prediction of energy costs associated to physical exercise, which will support the approach taken for the prototype development.

1.1 Energy expenditure measurement methods

For better control of the energy intake in high-performance athletes, patients with health problems or even for the population in general, appropriate dietary plans should be formulated. Therefore, it is extremely important to determine, as accurately as possible, the total energy spent by those individuals. The assessment can be done by various methods, each of them having "strengths" and "weaknesses". Some are summarized in table 1.1.

Method	**Advantages**	**Limitations**
Doubly Labeled Water (DLW)	High accuracy; Allows freedom of activity to participants	High cost; Qualified personnel required; Does not provide real-time data, neither specific details on the PA
Direct calorimetry	High accuracy	High cost; Subject confinement required for 24h or more
Indirect calorimetry	High accuracy; Provides data on the metabolic fuels being combusted	High cost; Qualified personnel required
Accelerometry	Non-invasive; Low burdensome to subjects; Inexpensive; Can be used anywhere; Provides real-time data	Inaccurate in predicting EE if used alone
Heart-Rate Monitoring	Low cost; Non-invasive; Versatile; Can be used anywhere; Provides real-time data	Inaccurate in measuring sedentary and light activities; Electrical and magnetic interference from common electrical devices
Pedometry	Inexpensive; Non-invasive; Provides real-time data	Limited to walking activities; Inaccurate in estimate distance covered and EE

Table 1.1: Methods to assess EE: reference methods include the Doubly Labeled Water technique, direct calorimetry and indirect calorimetry; indirect methods include accelerometry, heart rate monitoring and pedometry [54].

Among the methods, Doubly Labeled Water is considered the gold standard technique due to its high accuracy, precision and ability to do assessments within long periods of time

(7-14 days) [20] . This approach is applicable to a wide variety of population, including pregnant women, infants, elderly people and professional athletes [38]. But, due to its high cost and because it does not provide specific information about the PA (e.g., intensity level), it is not commonly used.

Another approach to assess EE is through calorimetry techniques. Direct calorimetry involves measuring directly the metabolic heat that is released by the body [43]. Due to its high cost and the impossibility of being carried out outside laboratory environments, it is almost never used in practice. On the other hand, indirect calorimetry is one of the most used methods to assess EE [68]. This technique estimates metabolic costs through the measurement of oxygen consumed and carbon dioxide produced, which results from the human energy metabolism production. This approach commonly serves as a reference method to assess the accuracy of other assessment techniques [61].

To overcome barriers, such as high cost or intrusiveness, possible solutions involve the indirect estimation of EE by measuring metrics correlated with it. For the past decades, accelerometry has gained popularity given its capability of being used for numerous physical activities. It is an objective, practical, and non-intrusive approach that can be used in either laboratory settings or free-living environments for various applications such as posture and movement classification [50] or metabolic cost estimation [12][15]. To improve the accuracy of physical activity classification or energy expenditure predicting models, accelerometry is frequently combined with other approaches, namely heart rate monitoring [13][35].

Heart rate monitoring is another example of an indirect, objective, non-invasive, and inexpensive method to assess EE both in laboratory and free-living environments [41]. This technique is commonly used to quantify intensity levels of physical activities due to the tight relation between heart rate and oxygen consumption, being extremely useful for EE estimations. Because heart rate is affected by factors unrelated with PA (e.g., emotional state), this technique has been used in conjunction with other assessment techniques, especially accelerometry [13][35].

Pedometry is a popular, inexpensive and non-invasive method commonly used by the population in general to estimate EE in activities such as walking or running [14]. By measuring the steps taken during motion, distance walked and EE can be estimated. However, the estimations given by these devices are most of the time erroneous and no information regarding the PA is provided.

Available devices for energy expenditure measurement, including the ones used in the methods previously mentioned, are presented in the following section.

1.2 Devices for energy expenditure measurement

A wide range of devices for direct or indirect energy expenditure measurement are currently available for different contexts. Some are summarized on table 1.2.

Name	Context	Data Recorded	Commercial Brands
Metabolic Gas Analyzers	Clinical; Research	Oxygen consumption, carbon dioxide production, EE	*Oxycon Mobile*, *Cosmed*
Accelerometers	Clinical; Research; Elite sports	Activity counts (amplitude and frequency of acceleration over each sampling period) and EE	*Actigraph*, *activPal*
Heart-Rate Monitors	Clinical; Social; Research	Heart rate and EE	*Actiheart*, *Polar*
Pedometers	Social	Steps taken and EE	*StepWatch-3*, *Yamax DigiWalker*
GPS Portable Devices	Elite sports	Distance covered, sprint distance, accelerations, EE, among others	*PlayerTek*, *StatSports*,*Catapult*
Armbands	Clinical; Research	Skin and near-body temperature, galvanic skin response and EE	*SenseWear*

Table 1.2: Devices available for EE estimation. Usage contexts, data recorded and commercial brands are presented for each tool.

Metabolic gas analyzers are tools used in indirect calorimetry techniques that measure oxygen consumption and carbon dioxide production to estimate EE. They normally consist in one or more portable processing units and a mask that covers the nose and mouth of the user to measure gases exchanges. In general, these tools deliver accurate results but are expensive and can affect the subject's natural behaviors while performing a workout [70].

Accelerometers are motion sensors that detect accelerations of body parts. These tools measure activity counts (i.e. amplitude and frequency of acceleration over each sampling period) in real-time and translate those counts into metrics of interest, such as EE. They are typically placed in locations that are close to the center of mass of the body, like the waist or lower back. Due to their low-cost, non-intrusiveness, simplicity and the inherent relation between movement and EE, accelerometers have been integrated in many studies where metabolic cost estimations were required [6][12][15]. In general, these are non-intrusive and cheap devices but may offer some limitations if not combined with other tools [69].

Heart-rate monitors are inexpensive and non-invasive tools used to estimate EE from heart rate measurements. They can provide real-time data on the frequency, duration, and intensity level of the PA executed. Typically worn on the chest (as an emitter) or on the

wrist (as a receiver), these devices allow comfort to the subject while performing any type of workout. Like accelerometers, heart-rate monitors can be combined with other devices to improve accuracy of energy cost estimations [38].

Pedometers are tools that estimate the distance covered and the energy expended by a person, by measuring the steps taken during the motion [23]. The simplicity and relatively low cost make these devices popular among the general population; also, nowadays many smartphones offer embedded pedometers thus making this technique almost ubiquitous. However, the estimates given by these devices are most of the time erroneous and limited information regarding the PA is provided.

GPS portable devices are nowadays used in a variety of physical exercises (e.g., football, rugby, rowing, triathlon) to predict a variety of metrics including distance covered, sprint distances, accelerations, EE, among others. The algorithms implemented on these devices are based on the bio-mechanical equivalence between accelerated/decelerated running on flat terrain and constant speed running uphill/downhill. Despite being scientifically approved, the algorithms do not take into consideration several factors, such as jumps, impacts or backwards running and, therefore, require deeper investigation [21].

Armbands are devices typically worn on the upper arm that capture signals from the environment to estimate EE using machine learning algorithms. These devices are commonly used in clinical context because they present high accuracy for light and sedentary activities. Armbands have also been worn by athletes to predict energy costs during the sporting season. However, its use in high intensity activities is still controversial, due to its inability to provide accurate values during high intensity levels. [45].

1.2.1 Choosing a device

The major factors that should be taken into consideration in the choice of a device for EE estimation are:

- Type of data intended to collect (e.g., heart rate, accelerations);
- Type of PA and its characteristics; this includes intensity levels, duration, frequency, environment locations (*indoor* vs *outdoor*), among others;
- Context in which the PA will be performed, e.g., predicting energy costs of paraplegic individuals during daily live activities, or estimating the energy expended by professional athletes during a football match;

- Product purchase budget;

- Specific limitations that may impact the accuracy of the prediction values (described in the previous section).

1.3 Models for energy expenditure estimation

Physical activity is a complex, mutable and multidimensional behavior, thus the accurate measure and quantification of energy expenditure associated to this component can be very challenging, specially if outside of laboratory environment. It is highly unlikely that a unique, "one-size-fits-all" model will ever be found that can be generalized for all types of activities and accurately estimate metabolic costs values. As technology advances, new and more accurate models are expected to be developed. The next subsections present some models used for energy expenditure estimation, including some mathematical models.

1.3.1 Equation of Weir

Indirect calorimetry is the most commonly used method to assess EE in both laboratory and field settings, because the portable measurement units used for measuring respiratory gas exchange allow relative freedom of movements. This technique relies on the fact that the human body consumes oxygen (O_2) and produces carbon dioxide (CO_2) to metabolize energy [36]. By measuring the volume of O_2 inspired and CO_2 expired, energy expenditure through indirect calorimetry can be estimated using the equation of Weir [10]:

$$EE = 3.9VO_2 + 1.1VCO_2 \tag{1.1}$$

- EE - energy expenditure, in kilocalories per minute ($kcal/min$);

- VO_2 - volume of consumed oxygen, in litters per minute (L/min);

- VCO_2 - volume of carbon dioxide expired, in litters per minute (L/min).

The complete form of this equation also uses urinary losses of nitrogen. However, this component can be ignored since no significant discrepancies were found between the results using the complete and simplified formulae [62].

1.3.2 Burn in Zone model

Burn in Zone is a model developed by S. Muangsrinoon et al. [53] to help people monitoring their heart rate while performing physical exercise, by establishing a relationship between the heart rate of the person and the correspondent performance level. This model was implemented on an Android application for a Huawei Smart Watch and also provides an estimation of calories burned during the exercise based on the average heart rate.

The Target Heart Rate Zone is shown on table 1.3 and defines the upper and lower limits of physical activity intensities. Each zone is based on the metabolic systems in the body that feed the muscles during exercise and separated according to the percentage of Physical Activity Intensity (PAI). Upper zones (Maximum and Hard) are related to anaerobic exercises, while lower zones (Moderate, Light and Very Light) are related to aerobic exercises. Anaerobic exercise is defined as *"an intense physical activity of very short duration, fueled by the energy sources within the contracting muscles and independent of the use of inhaled oxygen as an energy source"*, e.g. sprinting, High-intensity Interval Training (HIIT) or power-lifting [56]. Aerobic exercise is *"any activity that uses large muscle groups, can be maintained continuously and is rhythmic in nature"*, e.g. cycling, running or swimming [56].

Zone	THR(%PAI*MHR)	Benefits
Maximum	90-100% of MHR	Develops maximum performance and speed;
Hard	80-90% of MHR	Increases maximum performance capacity;
Moderate	70-80% of MHR	Improves aerobic fitness;
Light	60-70% of MHR	Improves basic endurance and fat burning;
Very Light	50-60% of MHR	Improves overall health and helps recovery;

Table 1.3: Target Heart Rate Zone.

For each zone, a range of Training Heart Rate (THR) values is defined. THR values, in beats per minute (bpm) are calculated multiplying the PAI percentage by the Maximum Heart Rate (MHR). The MHR is calculated using Tanaka's formula [34]:

$$MHR = 208 - (0.7 \times age). \tag{1.2}$$

The Caloric Expenditure (CE), given in $kcal/min$, is estimated by using the one of models developed by Keytel et al. [44]. The formula (1.3) is for male individuals and the formula (1.4) is for female individuals:

$$CE = (-55.0969 + (0.6309 \times hr) + (0.1988 \times w) + (0.2017 \times a))/4.184, \tag{1.3}$$

$$CE = (-20.4022 + (0.4472 \times hr) - (0.1263 \times w) + (0.074 \times a))/4.184, \quad (1.4)$$

where hr is the heart rate expressed in bpm, w is the weight expressed in pounds and a is the age expressed in years.

1.3.3 Machine learning approaches

Many studies in the fields of physiology, sports, and clinical nutrition have been made in order to obtain estimates of energy costs using wearable sensors during various types of physical activities. The signals provided by sensors are commonly used as inputs to black-box algorithms (e.g., multiple linear regression, neural networks, random forests) in order to predict instantaneous metabolic cost or the Metabolic Equivalent (MET) for a specific task.

Regression models based on simple and multiple linear regression have been commonly used for the prediction of EE, due to their simplicity and low computational cost. Keytel, et al. [44] developed multiple linear regression models that estimate EE based on heart rate and personal information (age, weight, and maximal oxygen consumption). Kimberly A. Ingraham, et al. [8] have used a multiple linear regression approach to predict instantaneous energy cost of individuals performing a variety of physical activities using physiological signals from different wearable sensors. Despite presenting reasonable results, this type of approach tends to overestimate or underestimate EE values, mainly during exercise intensity changes.

Neural networks have been also used for EE estimation. Firstbeat Technologies Ltd developed a model that uses an artificial neural network to estimate EE based on heart rate [48]. Neural networks have also been used in other configurations, for instance in generalized regression (Lin et al. [46]) and multilayer perceptron forms (Gjoreski et al. [32]), to predict EE. These type of models normally present better accuracy when compared to regression equations, because their estimation errors are significantly lower.

Branched regression models, such as decision trees (Ermes et al. [26]) and random forests (Ellis et al. [25]), have been developed for improving EE estimates. In general, the use of this type of models also showed improvement in the overall EE estimation accuracy.

In addition to the previously mentioned models, other approaches, such as Support Vector Machines or Hidden Markov Models, have been used for activity recognition to help improving EE estimation [47].

1.4 Objectives and contributions

The majority of devices currently available on the market for human body EE estimation present some limitations [38] [45]. The understanding of relationships between several physiological variables (e.g. heart rate, body accelerations) and EE can be the key to figure out what is missing on commercial tools and consequently minimizing the inaccuracy of the estimated values. Therefore, the main goal of this dissertation is to understand already known relations between physiological variables and EE and, if possible, discover new ones to develop and validate a low-cost wearable energy meter prototype of the human body, based on the use of multiple sensors and sensor fusion methods. The prototype should be easy to use, low-cost, non-intrusive, and provide real-time information to the user. The development of the prototype has been carried out in collaboration with Sports Science experts affiliated with Faculdade de Ciências do Desporto e Educação Física - Universidade de Coimbra (FCDEF-UC), both in the design and validation phases of the project.

1.5 Outline of the dissertation

The current document is organized in 5 chapters. After this introduction, chapter 2 presents some theoretical fundamentals associated to EE. Chapter 3 presents the study design and describes the EE measurement approach chosen. Chapter 4 describes the hardware and software implementation for the energy meter prototype. Chapter 5 addresses the main conclusions drawn from this dissertation and possible future work.

2 Fundamentals

In this chapter, some theoretical fundamentals related to energy expenditure measurement are presented. It is described the meaning of energy expenditure, its components and metrics that affect this variable. Some metrics correlated with energy expenditure and their impact on energy costs are also explored.

2.1 Terminology

Energy expenditure, physical activity and exercise are terms that describe different concepts. Energy expenditure can be *"considered a process of energy production from energy substrates (carbohydrates, lipids, proteins and alcohol) combustion, in which there is an oxygen consumption and carbon dioxide production"* [66]. During this process, part of the energy is lost as heat or urine and the remaining is stored in molecules known as adenosine triphosphates (ATPs). These molecules are responsible for providing the energy required for all muscle movements, heart beats, nerve signals and chemical reactions inside the human body [18]. According to Caspersen et al. [16], physical activity is defined as *"a bodily movement resulting from contraction of skeletal muscle that results in an increase in energy expenditure above resting levels"*. It can be quantified in terms of intensity (*how hard?*), duration (*how long?*), frequency (*how often?*) and type (e.g., walking, running, swimming...). Exercise is defined as a planned, structured, and repetitive movement with the goal of maintain or improve physical fitness [16]. Although they look similar, these terms have different meanings and should not be used interchangeably.

Energy expenditure can be expressed in terms of liters of oxygen consumed per minute ($L.min^{-1}$), milliliters of oxygen per kilogram of body mass per minute ($mL.kg^{-1}.min^{-1}$) or Metabolic Equivalents (METs). MET is a physiological measure that is used to represent the intensity of the physical exercise, ranging from 0.9 (sleeping) to 23 (running at a very fast pace). For instance, a physical activity equivalent to 4 METs requires the body to use 4

times more oxygen compared to a body at rest. For an average man at rest (sitting quietly), one MET equals approximately 250 $mL.min^{-1}$ of oxygen consumed, and for an average woman, 200 $mL.min^{-1}$. An accurate classification that considers variations in body size expresses METs in terms of oxygen consumption per unit of body mass, where 1 MET $\approx$ 3.5 $mL.kg^{-1}.min^{-1}$. [51]. Lists of energy expenditure estimations that express MET values for numerous physical activities have been developed and published in a Compendium [22][39].

2.2 Components of total energy expenditure

Total Energy Expenditure (TEE) refers to the total amount of energy expended during a 24h-period [38]. Figure 2.1 presents the components of TEE and some assessment techniques to quantify those components.

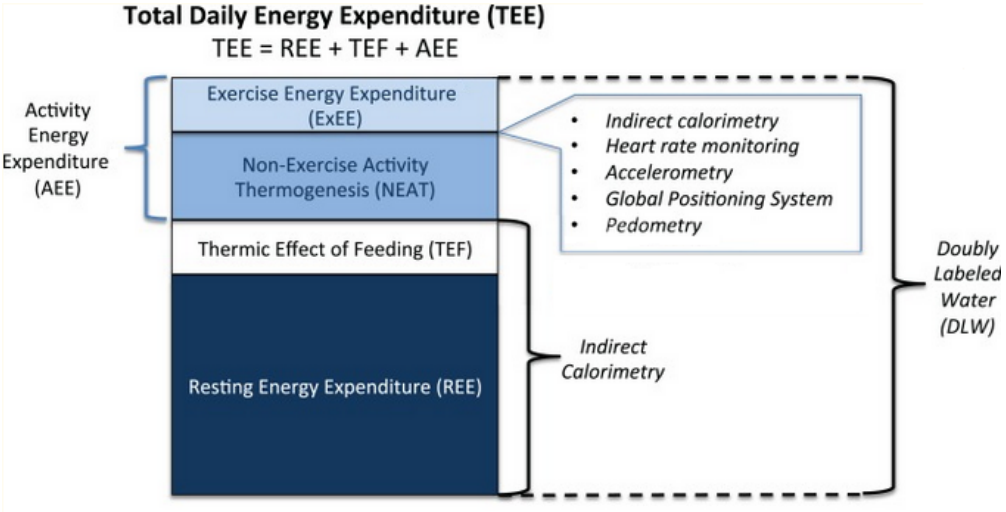

Figure 2.1: Total Energy Expenditure components and measurement approaches (reproduced from [38]).

TEE is composed by three major components:

- Resting Energy Expenditure (REE): the energy expended by an individual at rest in a thermo-neutral environment (e.g., energy costs of processes essential for life like breathing, sleeping, ...). Represents approximately 60-75% of TEE. Major factors that contribute to variations in REE on individuals include age, gender, body composition, body size, level of fitness activity and a range of genetic and environmental influences [58];
- Thermic Effect of Feeding (TEF): the energy required for the food digestion, absorption, transport and metabolism, storage of nutrients, and elimination of wastes. Represents approximately 10% of TEE [58];

- Activity Energy Expenditure (AEE): composed by the Exercise Energy Expenditure (ExEE) and the Non-exercise Activity Thermogenesis (NEAT). Ranges approximately from 15% (sedentary people) to 30% (athletes) of TEE. ExEE is the energy expended above REE and TEF due to muscular activity and physical activity related to sports-like exercises. NEAT is the energy expended for everything that is not sleeping, eating or sports-like exercise (e.g., walking to work) [7] [58].

2.3 Factors affecting energy expenditure

The accurate estimation of EE associated to physical exercise is influenced by several factors [40][38], standing out:

- **Individual characteristics**. This includes weight, age, gender, body composition, health, training level, emotional state, among others.
- **Physical activity characteristics**. Includes type, duration, frequency and intensity.
- **Environmental conditions**. Many physiological variables (e.g., heart rate) are affected by environmental conditions such as air temperature, altitude, humidity or barometric pressure, consequently affecting EE.
- **The REE component**, i.e. the energy required to keep the body functional at rest.

2.4 Metrics related with energy expenditure

The next subsections summarize some metrics related with EE.

2.4.1 Oxygen and carbon dioxide

Oxygen and carbon dioxide are arguably the physiological variables that most strongly correlate with EE. During the process of energy expenditure, the production of energy that involves the combustion of fuels carbohydrates, proteins, lipids, and alcohol requires the consumption of oxygen and carbon dioxide production. By measuring the volume of oxygen consumed and the volume of carbon dioxide produced, EE can be predicted. These gases are usually measured with portable metabolic analyzers that can be used both under free-living and laboratory conditions during indirect calorimetry approaches. EE is typically estimated by using the equation of Weir (see section 1.3.1).

VO2max

The aerobic fitness of an individual may affect his/her EE during physical exercise. The aerobic fitness of a person is related to his/her ability to perform moderate to high PA with large muscle groups for long periods of time [49]. The fitness level of an individual is usually indicated by his VO2max, i.e., the maximum amount of oxygen utilized by the individual, typically over two to three minutes, during an intense, maximal effort ($ml/kg/min^{-1}$). A variety of methods have been developed to assess VO2max. The most reliable methods are based on the linear relationship between oxygen uptake (VO_2) and power output, and between VO_2 and heart rate during exercise. Non-exercise estimates of VO2max have also been used, and are based on variables such as age, gender, body max, body composition, or heart rate. All these methods have advantages and limitations, and some are summarized in table 2.1.

Test	**Advantages**	**Limitations**
Direct VO2max laboratory test	The most accurate test, since it measures maximal oxygen consumption through gas analysis	Expensive, requiring confinement; Qualified personnel required; Only suitable for healthy individuals; Motivation to "reach the limits" can impact the results
Indirect submaximal (treadmill, cycle ergometer, step test)	Good accuracy; Cheap; Safer, has does not require maximal effort	Controlled protocol required; Accuracy is dependent on the accuracy of the maximal heart rate estimation
Cooper's 12-min test / 1.5-mile test and others	Acceptable accuracy; Can be performed on the field; Can be administrated to a large number of individuals at the same time	Maximal effort required; Only applicable for fit and healthy individuals; Motivation and pacing can impact the results
Walking tests (e.g. UKK 2km test, Rockport 1 mile test)	Can be performed on the field; Can be administrated to a large number of individuals at the same time; Safe	Low accuracy, especially for very fit persons; Motivation and pacing can impact the results; Distance must be measured accurately
Resting heart rate	Does not require physical exercise	Low accuracy; Does not have solid physiological basis
Firstbeat VO2max real-life estimation	Good accuracy; Cheap; Does not require maximal effort; Works on freely performed every day exercise	Exercise conditions should be standardized (for instance, running surface and wind may affect the result)

Table 2.1: Methods used for VO2max estimation (adapted from [49]).

2.4.2 Heart rate

A major factor that influences the EE associated with PA is the intensity level. Intensity is the requirement that an exercise is performed concerning the maximum possible capacity of the individual at a given moment, and can be evaluated according to biological responses, such as heart rate (HR). The necessary physiological adaptations to different distances demand different training intensities, and consequently different muscular needs. The identification of different intensity zones that express different energy consumption requirements of the muscular and cardio-respiratory systems can be made based on heart rate. Table 2.2 identifies intensity levels based on heart rate for cyclic sports.

Intensity Level	Heart Rate (bpm)	% Relative to MHR	Duration
Low	130-140	30-49	30 min
Medium	141-150	50-59	6-30 min
Sub-maximal	151- 165	60-74	1-6 min
Maximal	165-180	75-85	15-60 sec
Supra-maximal	<180	85-100	1-15 sec

Table 2.2: Intensity levels based on heart rate for cyclic sports (adapted from [60]).

Heart rate is one of the most used indirect parameters for EE estimation, because it is easy to measure, and the relation HR-EE is relatively accurate in steady state conditions. Moreover, heart rate monitoring is a cheap method that can be used under free-living conditions.

2.4.3 Accelerometry

Accelerometry is frequently used to predict energy costs associated to physical activities. Because acceleration is proportional to external force, it can reflect intensity and frequency levels of human body movements. Acceleration is commonly measured by accelerometers, simple and low-cost sensors that can be distributed over the body without causing significant restrictions to the subject movements while performing a workout.

To measure whole-body movement, motion sensors are typically placed as close as possible to the center of mass of the body. Ideal locations include waist, hip, and lower back. The sternum can also be considered a valid option since the torso occupies a major mass of the human body. Besides minimizing discomfort and constraints in body movements, the placement of motion sensors on these locations can also reduce external vibration and the gravitational effect that occurs during the execution of the workout. These are also regions

where it is easy to attach sensors, preventing relative motion between the tool and the body which can help mitigate noise in the signals acquired. Accelerometers can also be attached to other locations such as wrists, thighs, calfs or ankles [69]. As for the quantity, no consensus has yet been reached on the ideal number of sensors to use.

2.4.4 Metabolic heat

Being able to monitor internal body temperature during exercise can be useful if one desires to evaluate metabolic energy costs. During exercise, the metabolic heat produced within the body and the consequent increase in body core temperature (operating temperature of the organism) stimulates physiological mechanisms of heat loss by the human organism. Excess heat is distributed over body regions by blood circulation and carried by conduction to the body surface, where, insulated by clothing, is lost to the surroundings by convection, radiation, and evaporation. Additionally, heat can also be lost by respiration. A summary of mathematical models developed by Dusan Fiala, et al. [29] to predict heat losses that occur in the above mentioned mechanisms is presented in appendix B.

2.4.5 Fatigue

The individual's fatigue level during exercise is a factor to be considered. Metrics such as blood lactate, blood oxygen saturation (SpO_2), and muscle oxygen saturation (SmO_2) can be good indicators to assess fatigue. Electromyography (EMG) is also a technique that can be used to evaluate the state of fatigue in a muscle.

Lactate

The production of blood lactate is a natural consequence of energy metabolism during intense efforts and its accumulation leads to the fatigue of the organism. The more intense and prolonged the exercise, the greater the probability of fatigue, and the measurement of lactate values can be used for its monitoring. Typically, lactate is assessed by collecting blood samples. The main disadvantages of this procedure are the inability of providing real-time values and the discomfort caused to the individual. More recently, non-invasive and flexible sensors have been developed that can measure lactate concentration through sweat [9][37], providing much more comfort to the person and the ability to record data in real-time.

Muscle oxygenation and blood oxygen saturation

During exercise, energy is supplied to the muscles by sugar or oxygen. Oxygen is carried from the lungs to the rest of the body by a protein in the red blood cells called hemoglobin. When the red blood cells circulate to the muscles during physical exertion, they become deoxygenated. Blood oxygen saturation (SpO_2) corresponds to the fraction of oxygenated hemoglobin relative to total hemoglobin (oxygenated and deoxygenated) and is normally evaluated in percentage. During exercise, normal values range from 95% to 100%. Muscle oxygen saturation, also known as muscle oxygenation (SmO_2) represents the balance between oxygen delivery and oxygen consumption in the working muscles. Different physiological responses can be observed during exercise including increasing, steady or decreasing of muscle oxygen saturation which varies according to the individual's training level and type of muscle involved [2].

Electromyography

Another alternative to evaluate local muscle fatigue is by means of electromyography (EMG). EMG is commonly used for muscle activity detection. However, this technique can also be utilized to indicate the state of fatigue in the muscles by detecting the electrical potential generated by muscle cells when these are electrically or neurologically activated. Monitoring changes in EMG signals (e.g., changes in amplitude) is a common way to evaluate fatigue levels in the working muscles [17]. The main disadvantage of this approach is that it is only possible to detect the electrical potential at the surface of the skin if using surface electrodes. Needles can be used to detect signals inside the muscle, but cause discomfort and its use in real-life conditions is impracticable.

2.4.6 Electrodermal activity

Electrodermal activity (EDA) is a property of the human body responsible for changes in the electrical conductance of the skin. These changes occur due to variations in the state of the skin's sweat glands. These glands are controlled by the sympathetic nervous system, which is responsible to stimulate actions, such as increase in heart rate, adrenaline or sweat rate, that allow the body to respond to stressful situations [19]. Changes in EDA are also associated to changes in physical workload [59]. Physical activity increases the body temperature, which leads to an increase in the sweating rate and, consequently, to an increase in EDA.

It is believed that the emotional state of an individual, namely stress, can have a significant impact on his physical performance and consequently on energy expenditure. Considered a good bio-marker to measure stress [31], EDA can be a useful parameter to assess emotional state in individuals during sedentary activities, since EDA responses in these situations are easy to measure and the sensors used to evaluate this variable cause minimal discomfort. As for activities with moderate or high intensity levels, EDA measures may offer some limitations, since it can be hard to obtain accurate values.

2.5 Summary

After reviewing the energy expenditure components, it is possible to verify the existence of several factors and metrics that can affect its determination during physical exercise. With so many approaches available, a prior analysis should be made in order to choose the most appropriate metrics to use, considering the context in which the measurement will be performed.

The next chapter exposes a possible approach for the measurement of energy expenditure during physical exercise, based on the factors and metrics previously discussed.

3 Design and Preliminary Validation of the Energy Expenditure Meter

For the development of the energy expenditure meter prototype, a critical analysis was carried out beforehand to choose the most suitable design. This chapter begins by describing the approach taken for energy expenditure measurement according to the conditions imposed by the three physical exercise use cases that will be introduced in this chapter: running, indoor cycling and CrossFit. For each exercise, the variables selected, the type, number, and location of the sensors used to measure those variables are analyzed, followed by a description of the method used for energy expenditure estimation. Subsequently, the experimental procedure executed for data acquisition and energy expenditure computation is described. This description includes the performed validation tests and the respective analysis of the results obtained. Further validation tests are reported in chapter 4, after the implementation of the final prototype with the chosen devices and the printed circuit boards designed for that final prototype.

3.1 Types of physical exercise considered

Three types of physical exercises for energy expenditure measurement will be considered in the validation of the prototype to be developed: running, indoor cycling, and CrossFit. These were selected since they present significant differences among themselves, namely when it comes to locomotion and type of body movements. Before presenting the proposed energy expenditure approach, a description and analysis of these exercises are presented in the following subsections.

3.1.1 Running

In general, running can be considered an aerobic exercise that helps improve one's physical and mental health. It requires the individual to be athletic and well trained, being a strategy often used during body weight management or on the prevention of cardiovascular diseases. According to the American College of Sports Medicine (ACSM), running speeds can be defined as approximately 9.5km/h[1] (kilometers per hour) or more. Speeds ranging from approximately 6.5 to 9.5km/h are classified as jogging speeds and speeds slower than 6.5km/h are classified as walking speeds [55]. These speeds were defined for the population in general, since the demarcation between jogging and running speeds are more related to the individual's physical level. A jogging speed for an athlete may represent a running speed for a common individual. The focus of this work is on jogging and running speeds.

3.1.2 Indoor cycling

Cycling is one of the best exercises for improving one's health and fitness as it demands effort from almost all major muscle groups from the body. Therefore, the interest in estimating caloric expenditure during this type of physical exercise becomes even more relevant. Several types of cycling include road cycling racing, mountain bike racing, artistic cycling, BMX racing, indoor cycling, etc. The focus of this work is on indoor cycling, which involves using a stationary bicycle in a closed environment.

3.1.3 CrossFit

CrossFit is a high intensity, functional training mode consisting of a mix of aerobic exercises (e.g., rowing, etc.) and body weight exercises (e.g., olympic weightlifting). It is a modality that increases core strength, cardiovascular and respiratory endurance, agility, flexibility, among others, and is also a good alternative to lose weight. Unlike regular gym, which involves slow movements, few repetitions, and the use of machines, exercises included in CrossFit are very intense, last longer, have less recovery time between them, and do not include the use of machines [28].

[1]The American College of Sports Medicine [55] defined the speed values in miles per hour: 4mph or slower for walking, between 4 and 6mph for jogging and faster than 6mph for running.

3.2 Proposed approach

Because it is dependent on several factors, the accurate measurement of energy expenditure related to physical exercise can be very challenging. With this work, it is intended to develop and validate a prototype for a wearable energy expenditure meter that meets the following requirements:

- Low-cost, based on the combination of multiple sensors for the measurement of variables related with EE, and on sensor fusion methods.
- Non-intrusive, to avoid injuries and restrictions on body movements during a workout.
- Easy to use, so it can be utilized anywhere, especially outside the laboratory environment.
- Provide real-time energy expenditure values.
- Suitable for multiple physical exercises.

The prototype is not intended to estimate energy expenditure for one specific physical exercise. Instead, it should be developed and adapted according to the type of physical exercise being executed. In order for it to be as embracing as possible, two modalities with a greater predominance of aerobic work, running and indoor cycling, and one modality with a predominance of both aerobic and anaerobic work, CrossFit, were selected. Running and indoor cycling allow the measurement of energy expenditure in different aerobic modalities that request different muscle groups, originating different physiological responses. CrossFit allows the measurement of energy expenditure not only in aerobic, but also in anaerobic conditions, since it is a type of exercise strongly differentiated from the previous modalities, involving a variety of body movements at different intensities.

The measurement of energy expenditure in the different physical exercises will be based on intensity levels, body movements, fatigue, and psycho-physiological data. As they differ from each other, the acquired information will vary from exercise to exercise, namely on the type and quantity of signals. Table 3.1 summarizes the main differences between the use-cases regarding thee characteristics and the signals acquired.

The approach to measure energy expenditure in each of these exercises is described with more detail in the following sections.

Physical exercise	Characteristics	Type of signals
Running	Exercise with aerobic work preponderance; It only involves the use of the body, with greater demand from lower body parts; Dynamic exercise	Intensity: heart rate; Body movements: accelerometry; Fatigue: muscle oxygenation; Psycho-physiological data: electrodermal activity
Indoor cycling	Exercise with aerobic work predominance; Involves the use of a stationary bicycle, with greater demand from lower body parts; Static exercise	Intensity: heart rate; Body movements: accelerometry; Fatigue: muscle oxygenation and blood oxygen saturation; Psycho-physiological data: electrodermal activity
CrossFit	Aerobic and anaerobic physical exercise; It only involves the use of the body, with full-body muscle demand; Static and dynamic exercises involved	Intensity: heart rate; Body movements: accelerometry; Fatigue: muscle oxygenation; Psycho-physiological data: electrodermal activity

Table 3.1: Chosen use-cases: characteristics and signals acquisition information.

3.2.1 Running

The study of the literature allowed to verify that running is a commonly used physical exercise for mathematical models validation as it is included in a variety of other physical exercises, although not always in a constant and rhythmical form. Since it is continuous and keeps intensity levels approximately constant, makes it easier to obtain accurate predictions. For the purpose of this work, running was performed on a flat surface with 1% inclination to simulate the air resistance that would occur in an outdoor environment [42]. Despite running speeds being defined as 9.5km/h or more, speeds lower than that threshold (classified as jogging speeds, (6.5 to 9.5 km/h) were also considered, to include energy expenditure measurements at slow speeds, since these are often performed in warm-up and recovery exercises during running training.

Intensity assessment

Knowing the intensity level of a physical exercise is crucial if one desires to obtain accurate estimates of metabolic costs. As mentioned in section 2.4.2, intensity levels can be identified by heart rate. During moderate physical exercise, linear relationships between heart rate and energy expenditure have been established, within a range of approximately 90-150 bpm [44]. Since running is included in this category, heart rate has a significant impact on caloric

expenditure estimation and its measurement is incorporated in the prototype. To monitor this component, it was decided to use a heart rate chest strap. The location of the device on the body is critical for getting good accuracy. The closer the device is to the heart, the greater the accuracy, hence the choice of the chest strap. Being a non-intrusive tool also contributed to its inclusion on the prototype. The forehead is also an option, but the accuracy in this region is questionable and may not offer comfort to an individual while performing a running workout.

Owing to the fact that heart rate is controlled by the nervous system, variations in heart rate can also be attributed to changes in emotional state or environmental conditions. To overcome this barrier, this variable is combined with others (presented next) that are used in the prediction algorithm for energy expenditure measurement.

Body movements evaluation

Given the relation between acceleration and energy expenditure, accelerometers were included in the prototype for the assessment of body movements in running. As there is still no consensus on the optimal combination of number of accelerometers and ideal locations, an attempt was made to include a suitable amount of sensors that is the least intrusive possible and does not cause restrictions on movements during a running workout.

Based on the principle that for whole-body movement detection the sensors should be placed in locations that are close to the center of mass of the body, one valid option is to place a sensor in the pelvic region. This is a non-invasive and stable location since it offers minimal discomfort to the user and prevents significant motion between the sensor and the body. Another valid option is to attach an accelerometer in the region of the torso, namely on the sternum, as it occupies a major mass of the body. The placement of the sensor in this location can be beneficial, for instance, to obtain information regarding respiratory rate.

Considering that major movements during running are executed by legs, accelerometers should be placed on the thigh and foot, both on one side of the subject (left or right). The placement of sensors in these regions can be beneficial to obtain information regarding the steps taken during a workout. The arms are also used for maintaining balance during the motion, hence motion sensors can be placed on the arm and hand of one side of the subject.

Metabolic heat

Due to the conditions during which this work was executed and the impossibility of developing suitable technology in time, the estimation of metabolic heat was discarded[2]. In order to obtain body core temperature estimates, it would be necessary to attach temperature sensors on the skin to measure its surface temperature. This would imply the development of adequate technology to not damage the sensors and integrated circuits, which would delay the work already planned. Besides, it was also impracticable to obtain heat loss estimates for some of the mechanisms mentioned in section 2.4.4 (e.g. evaporation, respiration), without the use of expensive and intrusive material.

Fatigue assessment

The fatigue level of the individual is a factor to be considered. Although there are not many studies that associate fatigue to the estimation of energy expenditure, it is believed that these may be related. Since the majority of the energy while running is consumed by lower-body parts, it may be pertinent to assess the state of fatigue in these regions of the body, for instance in the thigh. For that purpose, the use of a muscle oxygen sensor (*Humon Hex* [3]) was recommended by Sports Science experts affiliated with FCDEF-UC. This tool measures muscle oxygenation on the muscle which is a good fatigue indicator. It should be placed on the subject's *vastus externus* (quadriceps muscle group) directly on the skin secured by velcro straps (Figure 3.1).

Figure 3.1: Humon Hex placed on the *vastus externus* [3].

The use of a pulse oximeter for blood oxygen saturation evaluation was discarded, due to the high risk of damaging the sensor while executing a workout. The use of EMG was also discarded because the only non-intrusive method of using surface electrodes is only capable of providing superficial muscle fatigue information. Besides, some studies have reported that during moderate and high intensity physical exercises, EMG signals are little or not affected [33]. Due to the impossibility of acquiring appropriate technology for measuring lactate in a non-intrusive way, its measurement was also discarded.

[2]Please take note that this work took place during the Covid-19 pandemic.
[3]`https://humon.io/`.

Psycho-physiological assessment

Since changes in EDA values are associated with variations in physical workload, an EDA sensor is used. The sensor electrodes apply a low constant voltage to the skin and record the electrical signal that represents the skin conductance variation. The electrodes are attached to the fingers or on the lower back.

3.2.2 Indoor cycling

The approach to indoor cycling is similar to the one used on running. Both can be considered aerobic, continuous, rhythmical and moderate physical exercises, although they develop different muscle groups that lead to differences in ventilatory responses, blood flow, and neuromuscular fatigue [52]. Among the existing types of cycling, indoor cycling was chosen as it is an activity performed in an indoor environment, facilitating the prototype validation process.

Intensity assessment

Indoor cycling can be considered an aerobic and moderate physical exercise and, for that reason, intensity levels must be evaluated to increase the accuracy of energy expenditure predictions. As in running, heart rate is the physiological marker chosen for the assessment of this component. For heart rate monitoring, a heart rate chest strap is included in the prototype. This tool was chosen due to its non-intrusiveness and accuracy. Like in the running approach, this variable is combined with other metrics (presented next) to mitigate the effects of emotional arousal and environmental conditions.

Body movements evaluation

Accelerometers are used to assess body accelerations during indoor cycling workouts. Since the majority of the movements come from lower-body members, it is pertinent to place accelerometers on locations such as thighs, calfs, and feet. Other locations such as sternum, pelvic region or lower back should not be discarded, as indoor cycling can also involve pedal standing actions that require the use of upper body parts, namely the torso. In the proposed approach, accelerometers should be placed on the sternum, pelvis, lower back, thigh, calf and foot, the last three on the same side of the body.

Metabolic heat

For the same reasons presented in section 3.2.1, metabolic heat loss estimation was discarded.

Fatigue assessment

During indoor cycling, the majority of the energy is consumed by lower body parts, i.e. by the legs. To assess local muscle fatigue in these members, a muscle oxygen sensor *Humon Hex* is included in the prototype. One of the goals pretended to be achieved with the incorporation of this sensor is to find eventual relations between fatigue and energy expenditure. The assessment of blood oxygen saturation is made by placing a pulse oximeter on the index finger. The use of electromyography and the measurement of blood lactate were not included, for the reasons previously mentioned (see section 3.2.1).

Psycho-physiological assessment

Similar to the approach designed for running, an EDA sensor is used due to the EDA's tight relation with physical workload. The electrodes of the sensor should be attached to the fingers or on the lower back.

3.2.3 CrossFit

Among the three activities listed, CrossFit is for sure the most challenging one when it comes to estimating metabolic costs since this type of physical exercise can involve both upper and lower body movements with multiple levels of intensity. The multitude of exercise types involved in CrossFit makes it difficult to generalize the calculation of energy expenditure during this modality. Unlike running or cycling, where the intensity levels stay approximately constant during the workout, sudden variations can occur while performing CrossFit workouts (with lifting or intervals) making the accurate measurement of energy expenditure more challenging.

Most of the algorithms developed so far focus on activities with approximately constant intensity levels, which may not be satisfactory to estimate values while performing CrossFit. Therefore, specific algorithms for each type of CrossFit exercise should be developed. The main challenge of this approach is to develop algorithms for non-steady state situations without the use of intrusive equipment.

Intensity assessment

CrossFit intensity levels vary depending on the type of exercise, hence the assessment of intensity levels through heart rate becomes a priority. The choice of the heart rate monitor to be used can be a bit delicate. The location that offers more accurate heart rate values is the chest, but the placement of a sensor in this location may interfere in some movements and cause discomfort to the subject during particular exercises. On the other hand, placing a sensor in the arm (e.g., a heart rate armband) or in the pulse (e.g., a heart rate fitness band) may be a less intrusive choice, but the accuracy of heart rate values can be questionable. For the purposes of this work, priority was given to obtaining accurate values, hence the use of a heart rate chest strap was chosen.

Body movements evaluation

CrossFit exercises in general involve the use of almost all body parts. Depending on the type of exercise, body movements can be executed synchronously or asynchronously by different members, with different intensities. For that reason, accelerometers can become very useful to assess body movements during CrossFit. The body parts where the devices are placed should also be taken into consideration to not affect the subject's movements or cause any injuries. In the proposed approach, accelerometers should be placed in two regions of the torso, including pelvis and sternum; three regions of the upper limbs, including hands, arms, and forearms; and in three regions of the lower limbs, including thighs, calfs, and feet.

Metabolic heat

For the same reasons presented in section 3.2.1, metabolic heat loss estimation was discarded.

Fatigue assessment

CrossFit exercises require explosive body movements. To reduce the risk of injury, the tools for the assessment of muscle fatigue must be non-intrusive and should have minimal interference with any type of movements. To that end, the use of a muscle oxygen sensor (*Humon Hex*) is a valid option, as it can be placed not only on the thigh, but also on the arm, with minimal interference. The pulse oximeter was discarded, because it causes discomfort to the individual while performing a workout and there is also a high risk of damaging the sensor. EMG sensors were discarded for the reasons previously mentioned (see section

3.2.1). Blood lactate measurement was also discarded because it was not possible to acquire an appropriate sensor for this purpose.

Psycho-physiological assessment

Similar to the previous approaches, an EDA sensor is used due to the relation between EDA and physical workload. The sensor electrodes should be placed on the lower back, to avoid injuries.

3.2.4 Energy expenditure estimation method using multiple linear regression

During the execution of a workout of any type of the previously mentioned exercises, energy expenditure measurements need to be accurate and computed in a comfortable and portable way. To meet these requirements, physiological signals provided by the portable devices mentioned in the previous sections are used, combined and integrated into black-box algorithms to predict energy expenditure. These algorithms weight the input variables in order to approximate a mathematical model of desired results.

Multiple linear regression models are used to estimate energy expenditure during running and indoor cycling. These were chosen, because at the time of this work, not enough data was acquired in order to apply more accurate approaches, for instance, neural networks. Nevertheless, this type of model delivers accurate results for steady-state conditions, i.e, when intensity levels stay approximately constant over time, being suitable for running and indoor cycling workouts. On the other hand, its accuracy for non-steady state conditions is questionable, which may not be satisfactory for CrossFit exercises. For this use-case, a reliable alternative would be to use a more accurate model, for instance a neural network or a random forest. However, these approaches require large amounts of data to deliver accurate results, which did not allow such implementation, as mentioned before. Therefore, multiple linear regression models were considered for CrossFit.

At the time of the realization of this work, it was not possible to obtain a reliable ground-truth. The initially planed ground-truth would be computed using the Weir equation (formula 1.3) through the analysis of gas exchanges. However, the Covid-19 pandemic situation did not allow the execution of this approach with the minimum safety and health conditions. Alternatively, it was suggested by Science Sports experts affiliated with FCDEF-UC to use the Firsbeat Technologies Ltd. model [48] that uses a neural network to estimate

energy expenditure based on heart rate. Unfortunately, neither the trained network nor the dataset used for training the network are publicly available. Therefore, energy expenditure values estimated by the Keytel et. al model [44] (approach used in the Burn in Zone model presented in section 1.3.2) were considered as a possible ground-truth and served as the target data, i.e. the energy expenditure aimed to be predicted. Despite presenting some limitations for being a linear regression model (for instance, underestimate values during changes in exercise intensity), this model was chosen because it is based on heart rate, a metric strongly related to energy expenditure.

Each multiple linear regression model is described by:

$$\hat{y}(t) = X(t)b, \tag{3.1}$$

where $\hat{y}\ (t)$ is the energy expenditure at time t (i.e, the ground truth), the vector $X(t) = [1\ x_1\ ...\ x_n] \in \Re^{n+1}$ contains an offset term and n sensor signals, and the vector b contains $n+1$ regression coefficients.

For the multiple linear regression analysis, the signals were divided into two categories: physiological signals, including heart rate, muscle oxygenation and electrodermal activity; and accelerometry signals, which provide information regarding accelerations from different segments of the body. In total, three five cross-validated multiple linear regression models were trained, containing: 1) the physiological signals, 2) the accelerometry signals, and 3) the combined signals (physiological + accelerometry). This distribution was made to discover which groups of signals have the best predictive capability to estimate energy expenditure. A five-fold cross-validation was made, in which the dataset was randomly divided into a training set (80%, containing training data, $\bar{X}$, and training targets, $\bar{y}$) and a testing set (20%, containing testing data, X', and testing targets, y'). For each cross-validation fold, the regression coefficients b where calculated through training data and training targets:

$$b = (\bar{X}^T\bar{X})^{-1}\bar{X}^T\bar{y}. \tag{3.2}$$

The predicted energy expenditure, $\hat{y}'$ was calculated by using the regression coefficients from the test data:

$$\hat{y}' = X'b. \tag{3.3}$$

The predicted energy expenditure, $\hat{y}' \in \Re^n$, and the ground-truth energy expenditure (i.e., the testing targets, $y' \in \Re^n$), where then compared by calculating the root mean square

error (RMSE):

$$RMSE = \sqrt{\frac{(y' - \hat{y}')^2}{n}}. \tag{3.4}$$

For each cross-validation fold, the mean absolute error (MAE) was calculated as:

$$MAE = \frac{|y' - \hat{y}'|}{n}, \tag{3.5}$$

At the time of this work, it was only possible to implement a model for running. In appendix C is presented the procedure for the development of the regression models for running.

3.2.5 Choice of sensor types and placement

The choice of the type and quantity of sensors, as well as their placement on the individual's body, was made in order to develop a non-intrusive prototype which has the ability to provide accurate information during the execution of each of the previously mentioned physical exercises. The chosen approach for each of the three activities is summarized in table 3.2.

Physical exercise	**EE model**	**Sensor**	**Quantity**	**Body location**
Running	Multiple linear regression	Heart rate monitor	1	Chest
		Accelerometer	5-6	Sternum, pelvis, arm, hand, thigh and foot
		Muscle oximeter	1	Thigh
		EDA sensor	1	Fingers or lower back
Indoor cycling	Multiple linear regression	Heart rate monitor	1	Chest
		Accelerometer	5-6	Sternum, lower back, pelvis, thigh, calf and foot
		Muscle oximeter	1	Thigh
		Pulse oximeter	1	Index finger
		EDA sensor	1	Fingers or lower back
CrossFit	Multiple linear regression	Heart rate monitor	1	Chest
		Accelerometer	12-14	Sternum, pelvis, hands, arms, fore-arms, thighs, calfs and feet
		Muscle oximeter	1	Thigh
		EDA sensor	1	Lower back

Table 3.2: Chosen approach for each of the three physical exercises: EE model, sensors, sensors quantity, and sensors placement on the body.

The next section describes the development and validation of the energy meter prototype.

3.3 Development process of the energy meter

The current section summarizes the practical and experimental component in this work. It presents all the stages and actions performed during the development of the energy meter prototype, including the experimental procedure performed for its validation.

3.3.1 Methodology

As mentioned in section 3.2, the study was based on three types of physical exercises: running, indoor cycling and CrossFit. Depending on the type of exercise chosen, the study variables, the sensors and their distribution over the subject's body were selected based on the literature review. From there on, validation tests were performed for data acquisitions. Data was later processed and used to develop the proposed model. Initially, it was planned to compare the results obtained by the proposed model with the reference methods, but due to the situation of the Covid-19 pandemic, such procedure was not possible. Alternatively, the proposed model was compared with other mathematical models found on the literature. To improve the accuracy of the model, some adjustments were made, namely regarding the type of study variables to use, and on the type, number and placement of the sensors on the subject's body. The development steps are illustrated by the flowchart shown in figure 3.2.

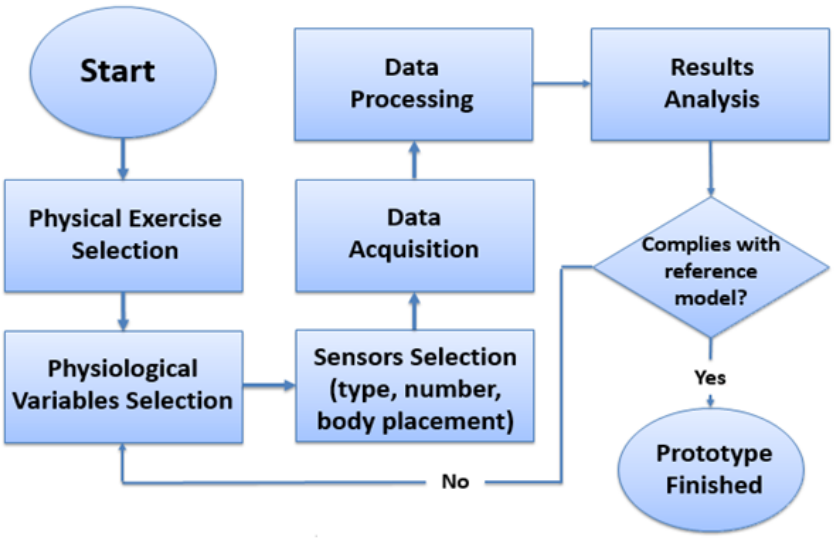

Figure 3.2: Diagram depicting the steps involved in the energy meter development.

The experimental procedure for the validation of the proposed energy meter prototype is presented in detail in the following subsections.

3.3.2 Preliminary work

In an earlier stage of the project, data acquisitions were carried out with a smaller prototype developed to demonstrate the practicability of the designed solution. This prototype was never aimed to be an earlier version of the final model, as it was only designed to collect data, and not to measure energy expenditure. The prototype contained a Kalenji Dual ANT+ / Bluetooth Smart Runner heart rate monitor belt, and a BITalino (r)evolution Plugged Kit BT containing a triaxial MEMS accelerometer and a SpO2 Reader (OSL) pulse oximeter (Figure 3.3). The BITalino (r)evolution Plugged Kit BT is a hardware board equipped with a micro-controller, UC-E6 cable connectors, and Bluetooth communication that allows the connection of multiple sensors for real-time data recording.

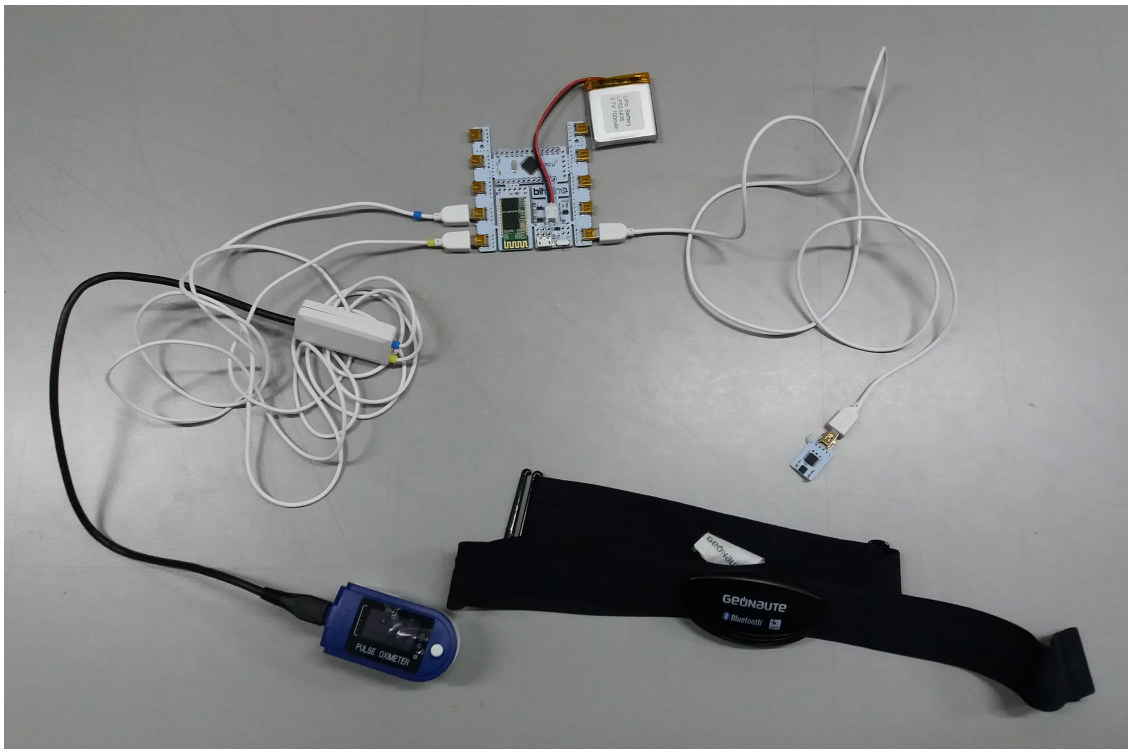

Figure 3.3: Preliminary setup.

The purpose of the first experiments was to obtain heart rate, body accelerations, and blood oxygen saturation percentage data from an individual running on a treadmill at different speeds, in a controlled environment. The MEMS accelerometer and the pulse oximeter were connected to the BITalino Kit via UC-E6 cables for real-time data recording. The MEMS accelerometer was placed on the subject's waist, the pulse oximeter on the index finger of the left hand, and the cardio band around the chest (Figure 3.4).

Figure 3.4: Accelerometer placed on waist and oximeter on the index finger (left). Cardio band placed on the chest (center). Preliminary experiment execution (right).

3.3.3 Experimental procedure

Of the three case studies, running was chosen for the validation the developed prototype. Due to the Covid-19 pandemic, it was not possible to perform experiments for all the three types of exercises, mainly due to the lack of time, and the impossibility of accessing the proper buildings and recruit volunteers to perform the experiments. Therefore, indoor cycling and CrossFit workouts were excluded. In the experiments described next, it was also not possible to implement the final version of the prototype that includes developed sensor boards for accelerometry data acquisition. Instead, an auxiliary tool was used to make up for the absence of the plates. It should be mentioned that this tool is not part of the developed prototype.

The experimental procedure is presented next.

Study sample

Twenty healthy subjects, seventeen males and three females with age (*mean* $\pm$ *standard deviation*): 21.3 ± 5.4 years, height: 1.74 ± 0.06 m, weight: 70.5 ± 11.0 kg, volunteered to participate in the experiments. Of the twenty participants, thirteen were athletes, three were moderately active (exercise three to four times a week), and four were poorly active (exercise two or less times a week). All participants signed an informed consent authorizing the collection of data during the experiments.

Protocol

The experiments were performed on a treadmill (Newfit, JS E4002), in a controlled environment (see figure 3.5). Subjects were randomly selected to participate in the morning

or in the afternoon. Before proceeding to the experiments, the participants were asked to complete a questionnaire regarding personal information (age, gender, height and weight), eating habits and other consumption, clinical history and physical activity level.

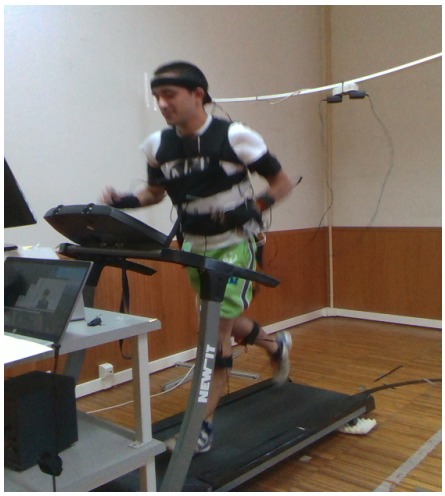

Figure 3.5: Subject running on a treadmill.

The experiments were divided into two categories, according to the person's physical activity level: athlete and non-athlete. The athlete experiment consisted of 2 minutes walking at 4km/h, 2 minutes running at 6.5km/h, 4 minutes running at 8km/h, 3 minutes running at 9km/h, 6 minutes running at 10km/h, and 3 minutes walking at 4km/h. The non-athlete experiment consisted of 4 minutes walking at 4km/h, 4 minutes running at 6.5km/h, 3 minutes running at 7.5km/h, 6 minutes running at 8.5km/h, and 3 minutes walking at 4km/h. Data was acquired between the fifth minute and the seventeenth minute. This time interval was considered as the "Test". A representation of the speed profiles for athletes and non-athletes is depicted in figure 3.7. Before starting the experiment, the participant was asked to lie down for 5 minutes, for resting heart rate data acquisition. The first minute was discarded.

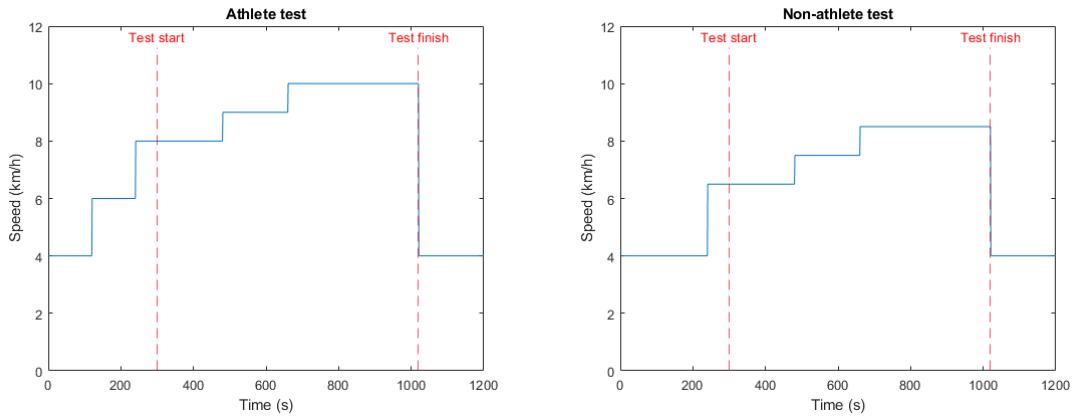

(a) Athlete test. **(b)** Non-athlete test.

Figure 3.6: Speed variation during the two protocols.

Appendix E contains a more detailed description of the protocol, as well as the informed consent and the questionnaire.

Wearable sensor recordings

During data collection, subjects were instrumented with a variety of sensors. Heart rate (in bpm) was measured using a Polar H7 (Figure 3.7a) heart rate monitor strapped around the chest. Muscle oxygenation (in percentage) was measured using the muscle oximeter Humon Hex[4] (Figure 3.7b) placed on the thigh secured by velcro straps. EDA (in Siemens) was measured by placing electrodes in the index and middle fingers of the left hand. For this purpose, a BITalino Kit (Figure 3.7c) was used. Subjects also wore a Xsens MVN inertial capture motion suit (Figure 3.7d), containing seventeen motion trackers that measure accelerations in x, y, and z axes, at 120Hz. The motion trackers were placed on the feet, lower legs, upper legs, pelvis, shoulders, sternum, head, upper arms, forearms and hands.

(a) Polar H7 heart rate monitor.

(b) Humon Hex oximeter.

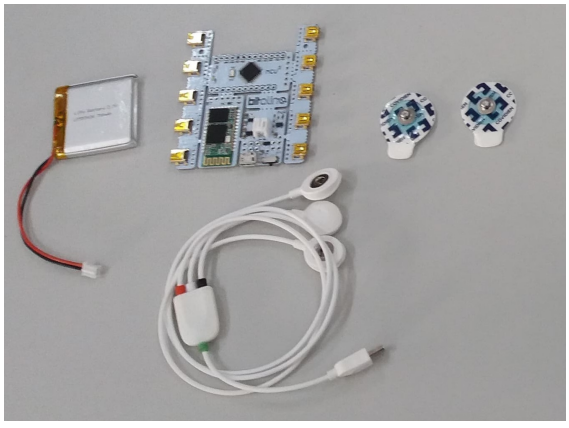

(c) BITalino Kit containing an EDA sensor.

(d) Xsens MVN suit.

Figure 3.7: Sensors used in the experiments.

The setup used in these experiments is presented with more details in chapter 4.

[4]This sensor was borrowed temporarily by a Sports Science expert affiliated with FCDEF-UC.

Signal processing

Accelerometer data from each of the three axis was band-pass filtered between 0.2Hz and 20Hz to remove the DC component and to isolate the dynamic component caused by body motion. The total acceleration was then determined by calculating the magnitude of the three axes, $M = \sqrt{a_x(t)^2 + a_y(t)^2 + a_z(t)^2}$. EDA data was filtered by using a low-pass filter, with a 1Hz cut-off frequency. All signals were downsampled to 1Hz.

3.3.4 Results

Of the twenty participants, only one did not complete the entire protocol. Due to equipment malfunction, some signals were also affected. In the sessions of participants 1, 2, 3, 4, and 5, data from the Xsens MVN suit was acquired with the occurrence of some frequency drops. In the session of participant 2, data from the Xsens MVN suit was not collected in the last 3 minutes and 9 seconds due to connection problems. The same has occurred for participants 6 (last 6 minutes and 22 seconds), 7 (first minute and 8 seconds) and 14 (entire test). During the sessions of participants 6, 10 and 15, the heart rate values were underestimated due to the probable misplacement of the sensor.

Heart rate

Figure 3.8 illustrates the plots of the heart rate measured at rest before the test (3.8a) and the heart rate during the test (3.8b) for one representative athlete subject. Figure 3.9 illustrates the plots of the heart rate measured at rest before the test (3.9a) and the heart rate during the test (3.9b) for one representative non-athlete subject.

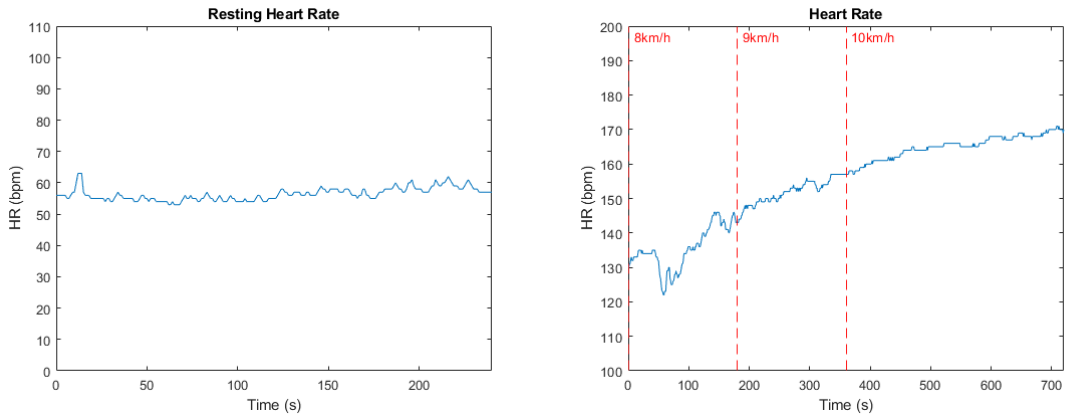

(a) Heart rate at rest measured before the test. **(b)** Heart rate during the test.

Figure 3.8: Plots of the heart rate measured before and during the test for a representative athlete subject.

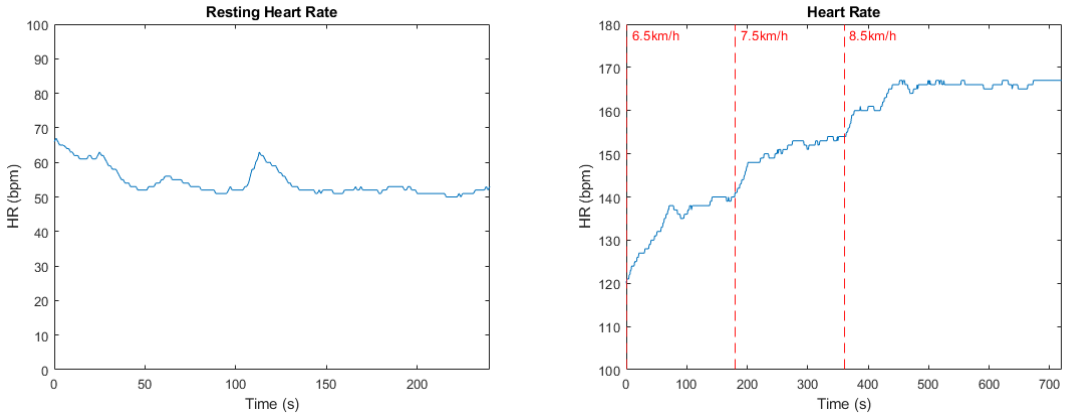

(a) Heart rate at rest measured before the test. **(b)** Heart rate during the test.

Figure 3.9: Plots of the heart rate measured before and during the test for a representative non-athlete subject.

The heart rate values measured during rest remain approximately constant over time. The occurrence of small variations can be justified due to the fact that the person was in a strange environment and knew that was being monitored. Such variations are typically more visible at rest.

In general, heart rate values increased throughout the test. It is possible to verify that the increase is significantly higher after a speed change. This happens because the body requires a higher amount of energy to accommodate new conditions. Muscles need more oxygen that is brought through the bloodstream, which implies an increase in heart rate. After approximately 1-2 minutes, the body is adapted to the new conditions, enters steady-state and the heart rate stabilizes. For the speeds used in the experiments, these variations are less evident in fit individuals as opposed to untrained individuals.

The heart rate values obtained are higher than expected for the intensities performed. This happens due to the fact that the MVN suit worn uses velcro straps that were tightly fastened to various parts of the subject's body. When compressed, the amount of blood that circulates in these areas is not enough to satisfy the needs of the muscle, which implies an increase in heart rate. This increase is more evident at higher intensities.

Muscle oxygenation

Figure 3.10 depicts the muscle oxygenation levels on the thigh of the right leg for both athlete (3.10a) and non-athlete (3.10c) representative subjects.

The Humon Hex sensor classifies the muscle as being in one of four zones:

- steady-state (green): the oxygen delivery and consumption in the muscle is balanced;

- approaching limit (orange): the muscle begins consuming more oxygen than what is being delivered;
- limit (red): the muscle is consuming significantly more oxygen than what is being delivered;
- recovery (blue): the oxygen delivery is greater than the consumption in the muscle.

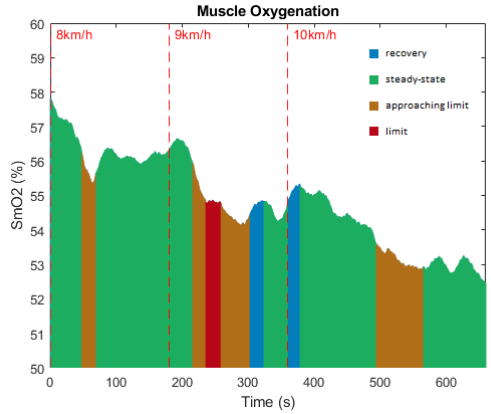

(a) SmO_2 percentage (athlete).

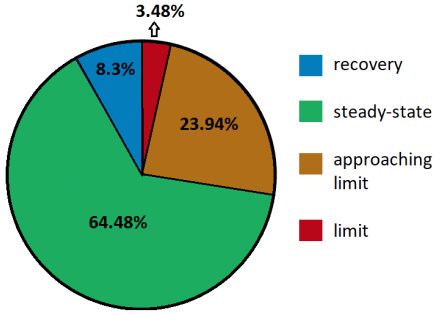

(b) Time percentage at each zone (athlete).

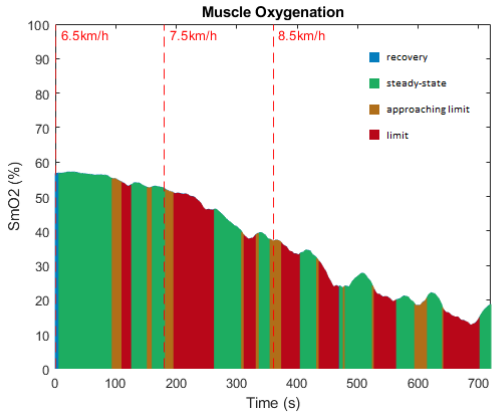

(c) SmO_2 percentage (non-athlete).

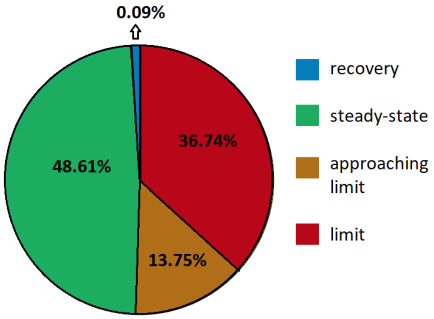

(d) Time percentage at each zone (non-athlete).

Figure 3.10: Plots of muscle oxygenation percentage. On the left, the variations over time during the test. On the right, the time percentages at each zone.

Muscle oxygenation levels can vary a lot depending on the individual's fitness level and type of workout. In the tests performed, there was a decrease in values over time, more pronounced in untrained individuals. It is possible to verify that after a change in speed, a decrease in SmO_2 occurs, sometimes reaching the limits of the muscle. When those limits are reached, some recovery attempts are made to try to reach steady-state. These attempts are more evident in athletes, since an athlete's body has a greater capacity for recovery as a result from his training, unlike an untrained individual. The time percentages at each zone are presented in figures 3.10b e 3.10d. As expected, SmO_2 limits were reached more

frequently and for longer periods in an untrained individual than in an athlete. It is also possible to observe that SmO_2 recoveries were practically non-existent in the untrained individual, which can be explained by his/her poor fitness and physical activity level.

Electrodermal activity

EDA filtered signals for both athlete (3.11a) and non-athlete (3.11b) representative subjects are presented in figure 3.11.

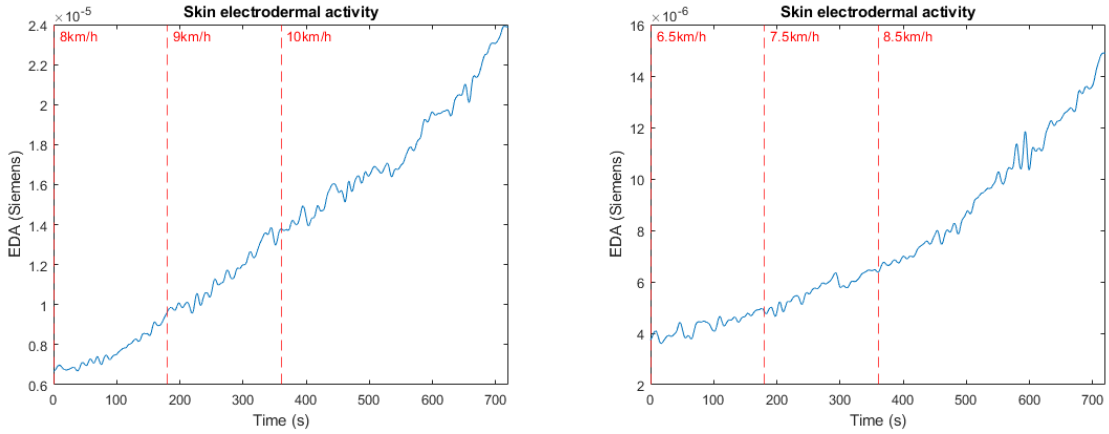

(a) EDA (athlete). **(b)** EDA (non-athlete).

Figure 3.11: Plots of EDA for athlete and non-athlete representative subjects.

The results show that EDA values increase over time, as expected. Typically, this occurs because the individual's sweat levels tend to increase as the exercise progresses.

Body accelerations

Magnitude accelerations from different body parts acquired with the Xsens MVN suit are presented in figure 3.12 for an athlete representative subject. Since no significant differences are verified between the acceleration values of an athlete and a non-athlete, the plots for a non-athlete representative were omitted. The plots of figure 3.12 illustrate a time interval of ten seconds at the highest speed (10km/h), for an easier interpretation.

Analyzing the plots, it is possible to verify a pattern of interval peaks with approximately constant duration. These peaks correspond to the instants when the foot hits the ground, allowing to estimate the number of steps taken during the test. This estimate can be easily made by overlapping the plots corresponding to the right foot and the left foot, where one step corresponds to the time interval between peaks, as shown in the figure 3.13. Knowing the speed s, in m/s, and the time interval Δt between peaks, in seconds (s), it is also possible

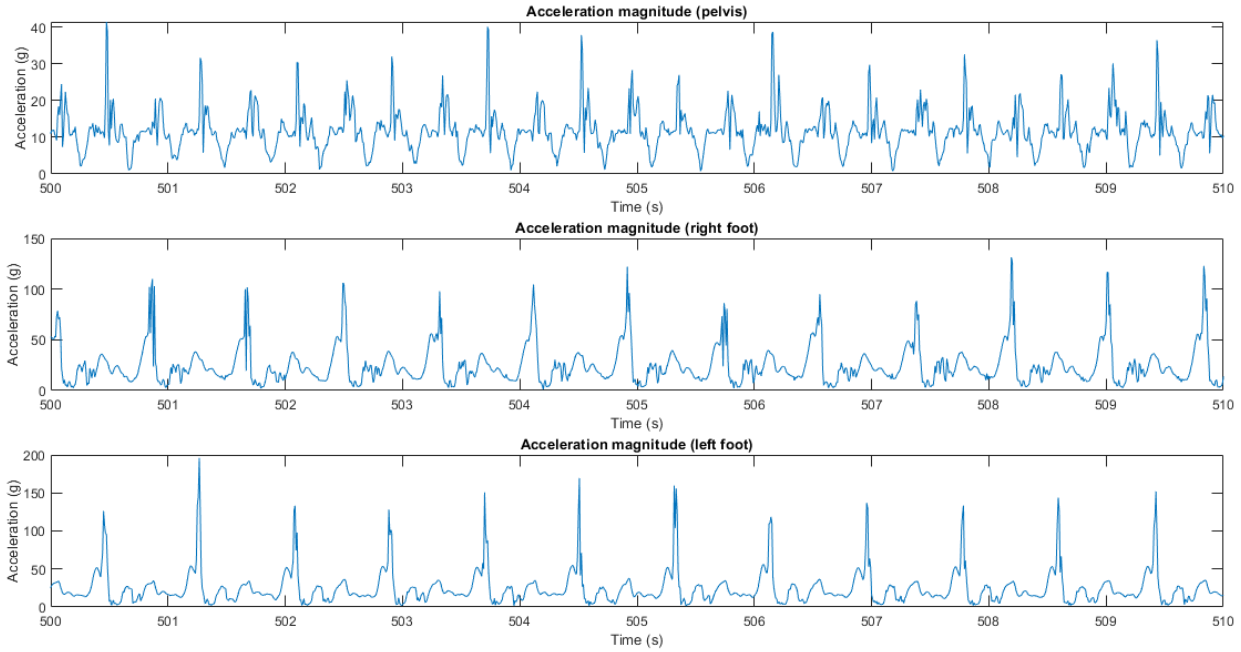

Figure 3.12: Magnitude acceleration of multiple body parts from an athlete representative subject. Depicted pelvis, right foot, and left foot.

to estimate the length of the step taken (l_{step}), in meters. For the step marked in figure 3.13 we have:

$$l_{step} = \Delta t \times s \Leftrightarrow l_{step} = (501.7 - 501.3) \times 2.78 \Leftrightarrow l_{step} = 1.11m \tag{3.6}$$

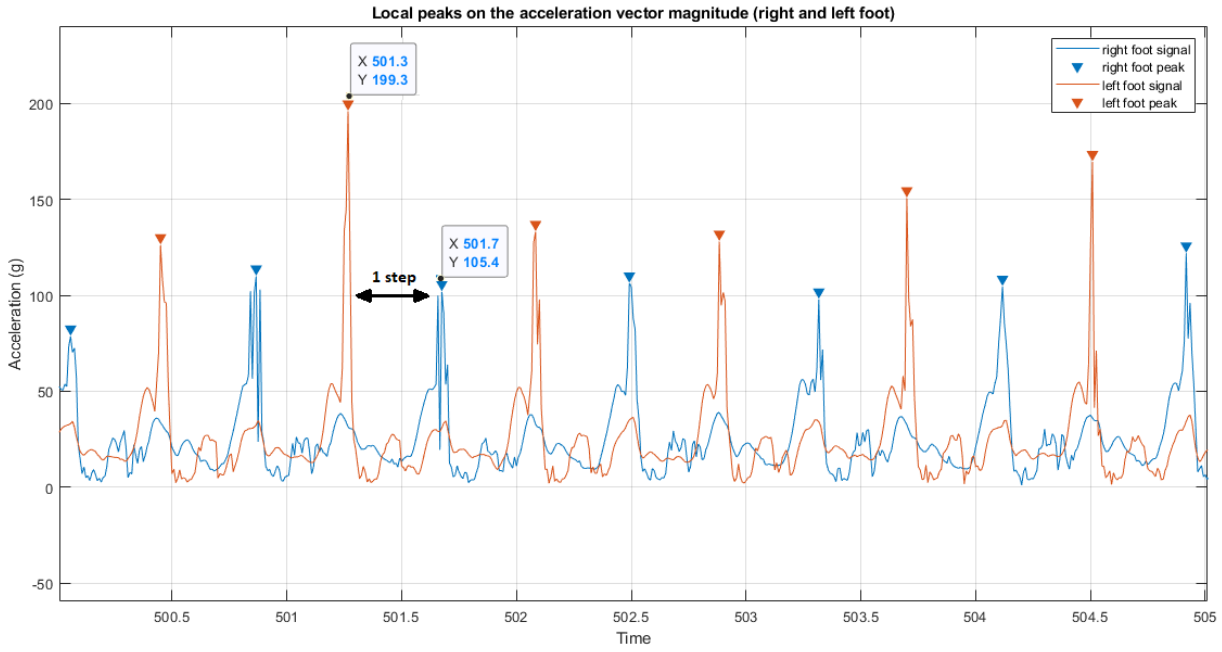

Figure 3.13: Depicted the magnitude acceleration of left foot and right foot, from one representative athlete subject. The time interval between peaks corresponds to one step taken.

Energy expenditure

The results of the multiple linear regression models to estimate energy expenditure from physiological data (heart rate, muscle oxygenation, and EDA), accelerometry data, and the previous combined, are presented in table 3.3. These models predict energy expenditure based on the model developed by Keytel et al. [44], since it was not possible to perform validation tests by using reference methods due to the Covid-19 pandemic that occurred during the execution of work.

Model features	Ground-truth EE (kcal/min)	Estimated EE (kcal/min)	RMSE (kcal/min)	MAE (kcal/min)
Physiological	13.4982 ± 2.5211	13.4983 ± 2.8414	1.0718 ± 0.0142	0.7439 ± 0.0088
Accelerometry	13.4982 ± 2.5211	13.4987 ± 2.0658	1.4474 ± 0.0228	1.0937 ± 0.0119
Combined	13.4982 ± 2.5211	13.4980 ± 2.4381	0.6422 ± 0.0144	0.4782 ± 0.0092

Table 3.3: Ground-truth EE, estimated EE, and error metrics for each multiple linear regression model (mean ± standard deviation).

The combination of signals led to a slightly better performance on energy expenditure estimation. The model that combines physiological and accelerometry data had the lowest RMSE (0.6422 ± 0.0144 kcal/min). On the other hand, the model that only contains accelerometry data had the highest RMSE (1.4474 ± 0.0228 kcal/min). The model containing only physiological data had a RMSE of 1.0718 ± 0.0142 kcal/min. To emphasize the signals correlation with ground-truth EE, figure 3.14 presents the processed signals along with the ground-truth EE, for both athlete (3.14a) and non-athlete (3.14b) representative subjects.

To evaluate the correlation between the considered EE ground-truth and each signal, Pearson's correlation coefficients were calculated using the MedCalc[5] software (see appendix C for a mathematical demonstration). The Pearson's correlation coefficient measures the linear correlation between two variables, ranging from -1 to 1. A value of -1 indicates a total linear negative correlation, while a value of 1 indicates a total positive linear correlation. A value of 0 means that there is no linear correlation between the variables considered. Table 3.4 presents the Pearson's correlation coefficients between the considered EE ground-truth and some of the signals acquired.

[5]https://www.medcalc.org/

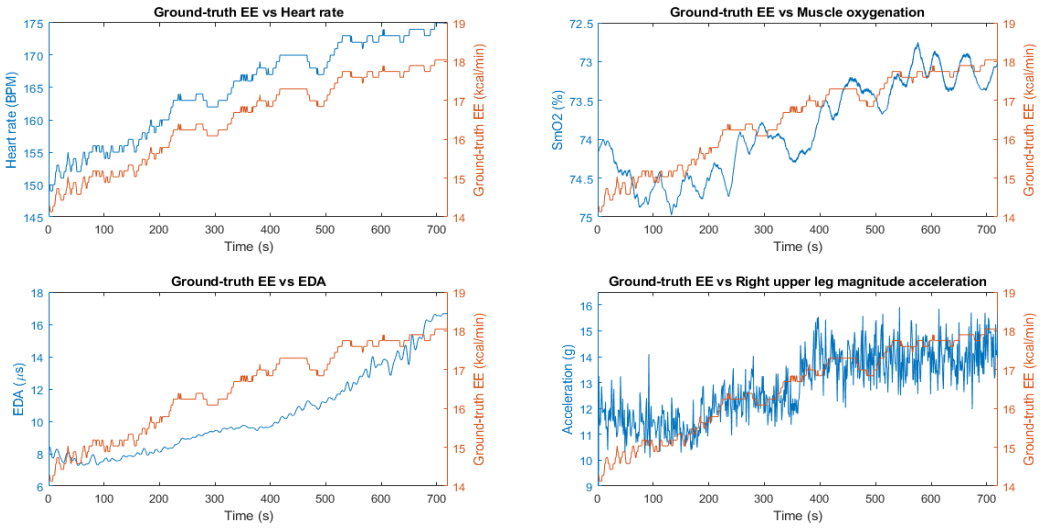

(a) Athlete representative subject.

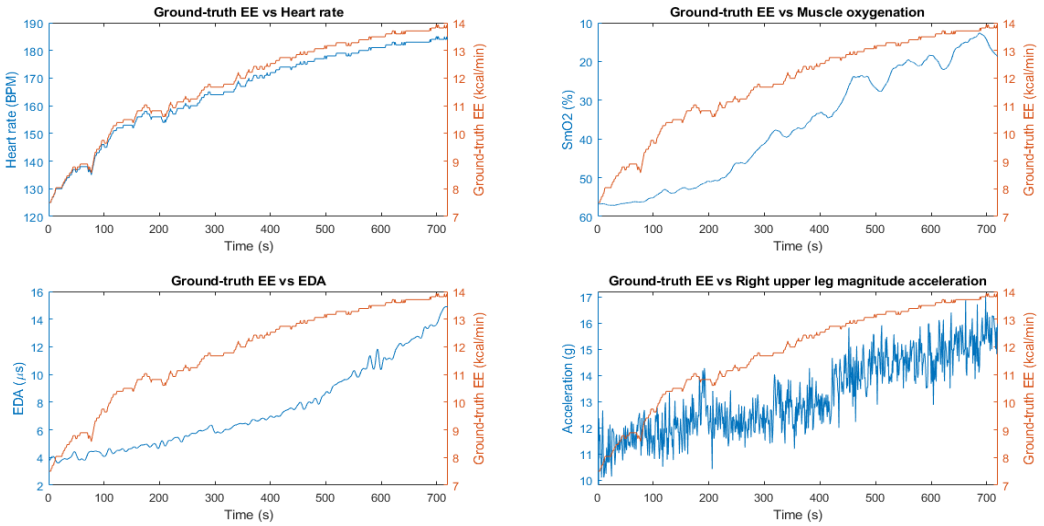

(b) Non-athlete representative subject.

Figure 3.14: Processed signals from an athlete representative subject 3.14a and a non-athlete representative subject 3.14b. Depicted, from top to bottom, heart rate, SmO_2, EDA, and right upper leg magnitude acceleration. Left axes refer to the signal, right axes refer to the EE ground-truth. Muscle oxygenation y axis is inverted due to its negative correlation with EE. The plots of the right upper leg (RUL) magnitude acceleration show the values resampled to 1Hz, for an easier interpretation.

Signal	HR	SmO_2	EDA	RUL magnitude acceleration
Pearson coefficient	1	-0.6883	0.8526	0.6717
$CI_{95\%}$	[1,1]	[-0.727,-0.646]	[0.831,0.872]	[0.627,0.711]

Table 3.4: Pearson's correlation coefficients with a 95% Confidence Interval (CI) between the EE ground-truth and some acquired signals: heart rate, SmO_2, EDA and right upper leg (RUL) magnitude acceleration.

3.4 Summary

The aim of this study was to develop and validate a prototype for a low-cost and non intrusive wearable energy meter. The developed prototype consisting of multiple sensors was designed and implemented based on three types of physical exercises, where appropriate sensors are selected according to the type of exercise performed. The signals acquired are processed and integrated into a multiple linear regression model that estimates the energy expenditure associated to the physical exercise performed.

Unfortunately, it was not possible to validate the prototype based on the reference methods, namely indirect calorimetry, due to the Covid-19 pandemic situation that occurred at the time of the execution of this work. Alternatively, it was suggested by Science Sports experts affiliated with FCDEF-UC to validate the developed model based on the one developed by Firstbeat Technologies Ltd [48], but since neither the trained model nor the dataset used for training are publicly disclosed, this approach was discarded. Consequently, the developed model was validated based on Keytel et. al model [44]. This approach presents some limitations, as this model is sample dependent and only provides accurate values for steady-state conditions, i.e., when the exercise is performed at a constant intensity level after one to two minutes of an intensity level change. Unfortunately, given the existing conditions at the time of the realization of this work, it is believed that this was the most convenient solution to use.

Due to the Covid-19 pandemic situation during the work, it was also not possible to implement the final version of the prototype in the experiments previously described. The final version, which is presented in chapter 4, contains developed sensor boards for the acquisition of accelerometry data. There was a delay in the delivery of these sensor boards that led to changes in the initially proposed plan. The accelerometry data from these boards would be used as a feature in the models developed for energy expenditure computation, but since it was not possible to acquire enough data, the Xsens MVN suit was used instead for the experiments reported in this chapter. Nevertheless, to demonstrate the practicability of the developed boards, experiments were made to compare accelerometry data acquire with the developed boards and with the Xsens MVN suit. These comparative results, as well as the final version of the prototype are presented in detail in the next chapter.

4 Implementation of the Final Prototype of the Energy Expenditure Meter

This chapter describes in detail the final prototype version for the energy expenditure meter. Initially, an overview of the prototype architecture is presented, followed by a depiction of the hardware and software implementation. Finally, the embedded system tests carried out for the validation of the developed prototype are presented.

4.1 Architecture overview

The architecture diagram of the developed setup is shown in figure 4.1.

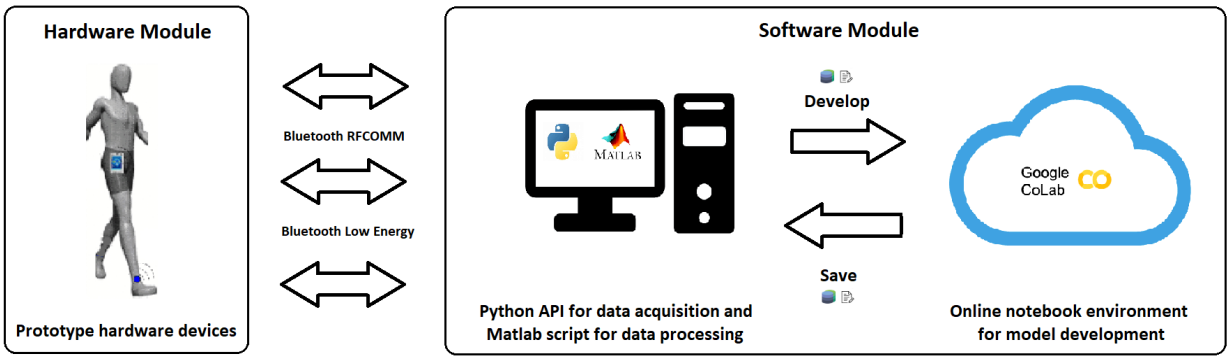

Figure 4.1: Architecture diagram of the energy meter prototype developed.

The architecture is composed by two modules: the *hardware* module and the *software* module. The *hardware* module contains the devices that integrate the developed prototype. The *software* module incorporates the code developed for data acquisition, data processing, and computation of energy expenditure. The communications between modules use Bluetooth, Radio Frequency Communication (RFCOMM), and Bluetooth Low Energy (BLE) protocols.

4.2 Hardware Implementation

4.2.1 *BodyEnergyExpenditure* prototype

The prototype was built to be as less intrusive as possible to not cause any movement restrictions and avoid injuries during the execution of the workouts. The hardware setup (Figure 4.4) consists in one Polar H7 heart rate monitor (Figure 4.2a), one muscle oximeter (Figure 4.2b), seven designed printed circuit boards (PCBs) (one primary board and six smaller boards, see Figure 4.2c), and one BITalino (r)evolution Plugged Kit BT (Figure 4.2d), containing an EDA sensor.

(a) Polar H7 heart rate monitor.

(b) Humon Hex oximeter.

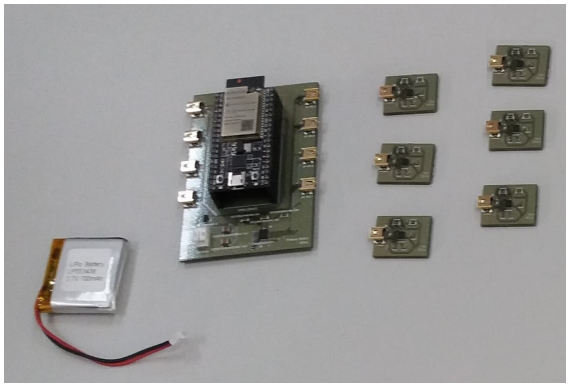

(c) Designed sensor boards.

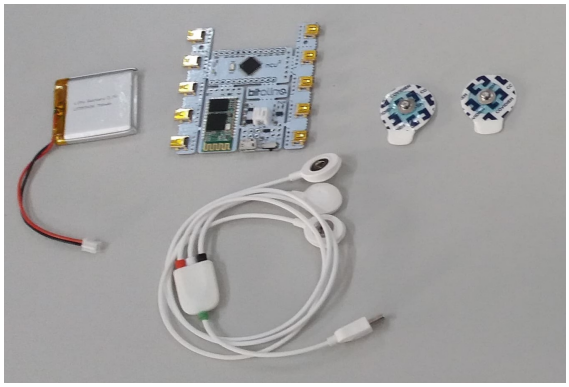

(d) BITalino (r)evolution Plugged Kit BT.

Figure 4.2: Setup used for the energy meter prototype.

BITalino devices

The BITalino (r)evolution Plugged Kit BT (Figure 4.3) incorporated on the prototype was used to collect data from an EDA sensor (Figure 4.3b). The EDA sensor is connected to the BITalino Core BT (Figure 4.3a) through a UC-E6 cable (Figure 4.3c). A 2-lead electrode cable (Figure 4.3d) is used to connect the EDA sensor to the electrodes (Figure 4.3e). The sampling frequency was set at 100Hz and the data was acquired through Bluetooth. All of these components were purchased in the course of this dissertation project and are commercially available. The total cost of this set of components is 130€.

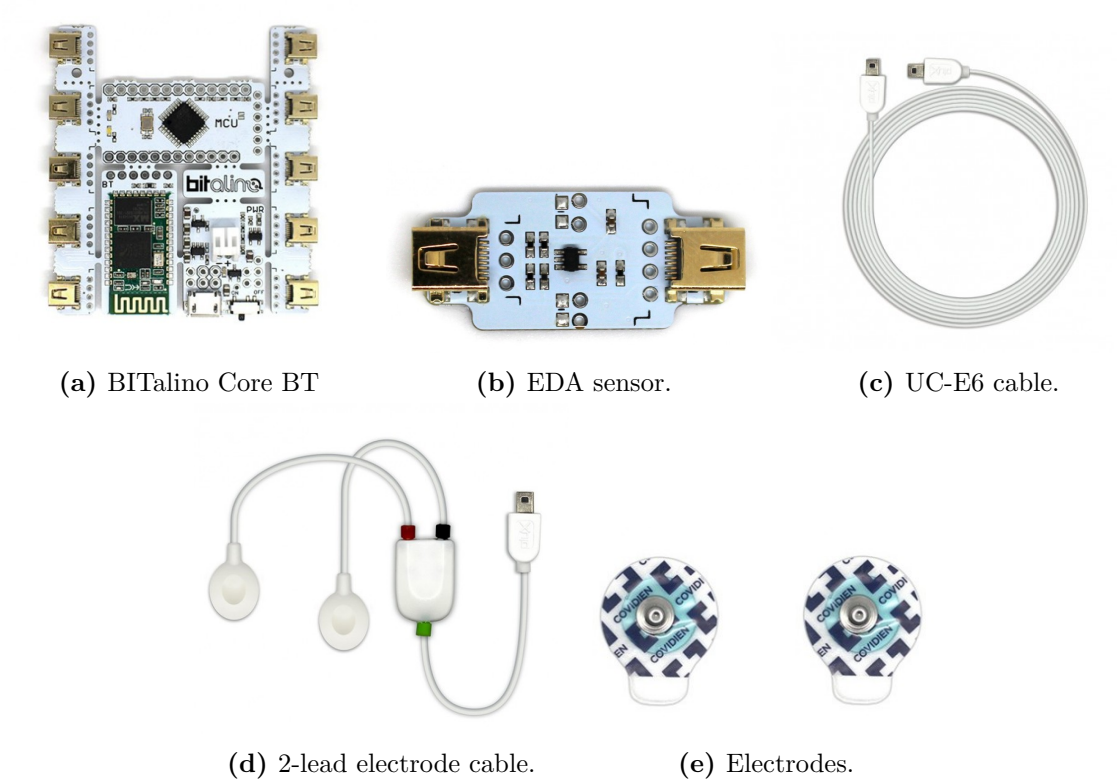

(a) BITalino Core BT **(b)** EDA sensor. **(c)** UC-E6 cable.

(d) 2-lead electrode cable. **(e)** Electrodes.

Figure 4.3: BITalino (r)evolution Plugged Kit BT. Presented BITalino Core BT (4.3a), EDA sensor (4.3b), UC-E6 cable (4.3c), 2-lead electrode cable (4.3d), and electrodes (4.3e) (Figures reproduced from [1]).

Designed PCBs

To acquire accelerometry data, two types of boards were developed: one primary board and six smaller boards (see Figure 4.4). These were only included in the final version of the prototype, at an ending stage of the work, which did not allow their use on the experiments described in section 3.3.3. The electrical schematic diagrams and the board designs of the designed printed circuit boards (PCBs) are presented in appendix A.

The primary board (Figure 4.4a) was designed to occupy the minimal PCB area possible. It contains the processing and communication modules, as well as a power unit, and incorporates one ESP32 micro-controller, one XC6220 voltage regulator, and one TCA9548A 8-channel I2C multiplexer.

The six smaller boards (Figure 4.4b) were also designed to occupy minimal PCB area, so that they could be easily attached to the individual and used during the workout (e.g. when running). Each board contains one ICM-20648 MEMS accelerometer sensor [64] and can be connected to the primary board via a UC-E6 cable. The number of smaller boards and the locations to place them on the subject's body vary according to the type of physical exercise performed, as discussed in sections 3.2.1, 3.2.2, and 3.2.3.

(a) Primary board.

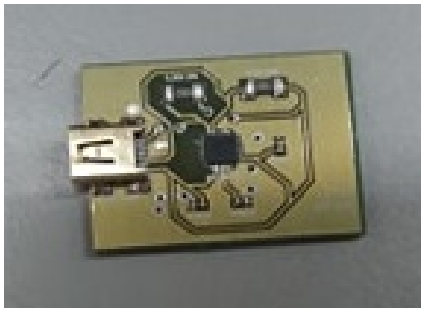

(b) PCB containing a ICM-20648 sensor.

Figure 4.4: Designed PCBs.

When using a single-power supply, the recommended operating voltage of ESP32 is 3.3V, and its recommended output current is 500 mA or more [27]. Therefore, each primary board is supplied by a LiPo battery with 3.7V of nominal voltage, regulated down to 3.3V by a XC6220 voltage regulator. The maximum output current of the XC6220 is 1000mA, which fulfills ESP32 minimum operational requirements.

To be able to read data from multiple sensors with similar I2C addresses, a TCA9548A 8-channel I2C multiplexer is used. As described in [64], in a generalized I2C interface implementation, attached devices can act as a master or as a slave. The master device puts the slave address on the bus, and the slave device with the matching address acknowledges the master. The ICM-20648 always act as a slave, and communicates with the ESP32 that acts as the master. Since multiple ICM-20648 sensors were used and it is only possible to assign two different addresses for each device, the TCA9548A 8-channel I2C multiplexer was used. This device contains 8 channels and each channel has one ICM-20648 connected. Any of the channels can be selected according to the programmable control register of the ESP32, which sends a byte of data to the TCA9548A's bus register corresponding to the selected channel, avoiding I2C slave address conflicts [65]. In the case where a slave device has the same address as the multiplexer, the TCA9548A has tree pins (AD0, AD1, and AD2) that can be used to change the default address. Such procedure was not required in the prototype described herein.

All the data read from the sensors of the smaller boards is transmitted to a computer through Bluetooth using RFCOMM protocol. Initially, data transmission via BLE was tested. However, there was a significant loss of packets when using this approach. This occurred because BLE is intended to use less power and only transmits short amounts of data when required, not being ideal for streaming applications [5].

The total cost of this set of components, including the designed PCBs and the UC-E6 cables that connect each smaller board to the primary board is 250€.

Heart rate monitor

A Polar H7 heart rate monitor (Figure 4.2a) was provided by a Sports Science expert affiliated with FCDEF-UC and is included in the prototype for heart rate data acquisition. Data from this tool was acquired through BLE. This device uses the Generic Attribute Profile (GATT), a protocol that defines how two BLE devices exchange data with each other using concepts called Services and Characteristics [5]. Services contain specific chunks of data called Characteristics. Each service is unique and has an Universal Unique Identifier (UUID) that can be either 16-bit (defined by the Bluetooth Special Interest Group (SIG)[1]) or 128-bit (for custom services). Characteristics encapsulate a single data point which contains the data to be read and, similar to Services, each Characteristic distinguishes itself via a pre-defined 16-bit[2] or 128-bit UUID [4].

The Services and Characteristics UUIDs of the heart rate monitor were initially unknown. Therefore, a scanning was performed to obtain the GATT Services and Characteristics compatible with the device. The official adopted service for heart rate (Heart Rate Service), which has a 16-bit UUID equal to 0x180D, was found to be compatible with the heart rate monitor. Consequently, the official Heart Rate Measurement Characteristic, with a 16-bit UUID equal to 0x2A37, was compatible with the device, allowing heart rate data acquisition from the heart rate monitor.

At the time of the purchase, the cost of this sensor was around 45€.

Humon Hex

To acquire muscle oxygenation data, a muscle oxygenation sensor Humon Hex (Figure 4.2b) is included in the prototype. This sensor was borrowed temporarily by a Sports Science expert affiliated with FCDEF-UC. At the time of the purchase, the cost of this sensor was around 250€.

Since this is a BLE device, a scan was performed to discover the Services and Characteristics UUIDs. Unlike the heart rate monitor, there is no official adopted service or characteristic for muscle oxygenation, which hindered the process of decoding the data. This was the chosen approach due to the fact that the company responsible for the manufacturing and maintenance of this device is no longer active. Fortunately, an online solution was found that allowed to identify the service and characteristic UUIDs that contained the

[1]Service UUID: `https://www.bluetooth.com/specifications/gatt/services/`.
[2]Characteristic UUIDs: `https://www.bluetooth.com/specifications/gatt/characteristics/`.

desired data and how to decode it [11].

To demonstrate the reliability of the SmO_2 data obtained, new experiments were made on a treadmill, in a controlled environment. SmO_2 data was acquired using a developed software (the one used on the experiments described in section 3.3.3) and the MoxZones mobile application[3], a commercial product that is used for SmO_2 data collection and analysis. Five subjects participated in the experiments. The tests were performed on different days, with a 48-hour interval each. One day data was acquired with the developed software and on the other day with the Moxzones mobile application. The days were randomly selected (acquisition with the developed software or with the Moxzones app). The tests were divided into 3 parts: rest, where the subject remained seated for 2 minutes; 6 minute warm-up (1 minute at 4km/h, 1 minute at 6 km/h, 1 minute at 7km/h, 1 minute at 8km/h, 1 minute at 9km/h, and 1 minute at 4km/h); and 5 minutes running at 10km/h. The results are shown in figure (4.5) for one representative subject.

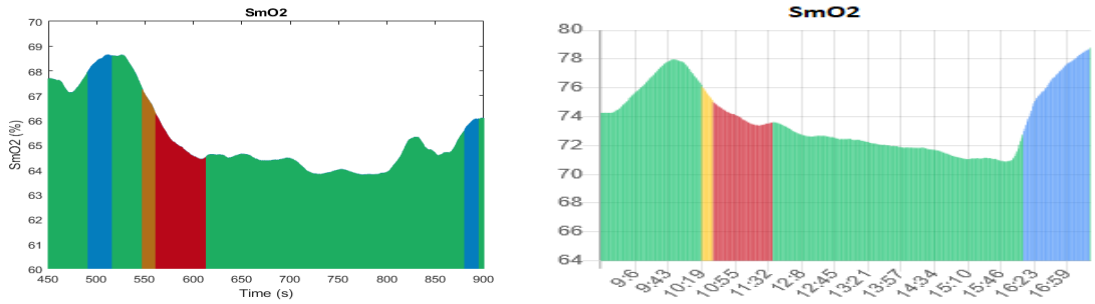

(a) Developed software SmO_2 data. **(b)** MoxZones App SmO_2 data.

Figure 4.5: Plots of SmO_2 data acquired with the developed software and with the MoxZones App, for one representative subject.

To measure the relationship between SmO_2 data acquired with the developed software and with the MoxZones App, the Intraclass Correlation (ICC) coefficient was calculated. ICC is a parameter that measures the correlation between two or more measurement samples of a quantitative variable. The calculation of this coefficient was made using the MedCalc software[4] (see appendix C for a mathematical demonstration).

Samples collected during the warm-up and the 10km/h run were considered. Since the developed software acquires data at a sample rate of 4Hz, mean values per second were considered. The ICC coefficient for the representative subject previously mentioned has a value of 0.9 (95% confidence interval: $CI_{95\%} = [0.878,0.918]$), indicating a strong correlation between SmO_2 data acquired with the developed software and the MoxZones App.

[3] `https://moxzones.com/`.
[4] https://www.medcalc.org/

4.2.2 Xsens MVN suit

At the time of this work, due to the Covid-19 pandemic, it was not possible to fully carry out the experiments initially planed, as mentioned in section 3.3.3, due to a delay in the delivery of the designed PCBs for accelerometry data acquisition. As an alternative, to capture the participant's body motion and acceleration data, a Xsens MVN inertial motion capture suit was used in the experiments presented in section 3.3.3. This suit consists of two Xbus Masters and seventeen inertial and magnetic measurement units that comprise 3D gyroscopes, 3D accelerometers and 3D magnetometers. The sensor modules connect to the Xbus Masters, which provide power, synchronize the sensors sampling and allow wireless communication with the PC. The sensors were placed on the feet, lower legs, upper legs, pelvis, shoulders, sternum, head, upper arms, forearms and hands. Since the initial pose between the sensors and body segments is unknown, a calibration procedure is required, in which the sensor to body alignment and body dimensions are determined. To perform the calibration, the foot length and height, in cm, are entered and the subject is asked to stand still with the arms down next to the legs (Figure 4.6).

Figure 4.6: Xsens MVN inertial motion capture suit consisting of 17 inertial and magnetic sensor modules. A calibration procedure is required to determine sensor to body alignment and body dimensions.

The cost of this suite is in the order of 10,000€, which is much higher than the cost of the designed PCBs (250€).

4.2.3 Accelerometry data comparison

Accelerometry data acquired with the accelerometers incorporated in the designed PCBs was not included in the developed models. Instead, experiments were made to compare the data acquired with the developed sensor boards and the data acquired with the Xsens MVN suit. The experiments were performed at an ending stage of the work, which did not allow to recruit the number of volunteers initially planned (e.g. 20 subjects as in the experiments reported in section 3.3.3). The only subject who participated in the experiments wore the Xsens MVN suit in conjunction with the designed PCBs. These were attached to the pelvis region, left forearm, left hand, left upper leg and left foot. The subject performed the athlete protocol used in the experiments described in the section 3.3.3. The plots of the signals are presented in figures 4.7, 4.8, and 4.9.

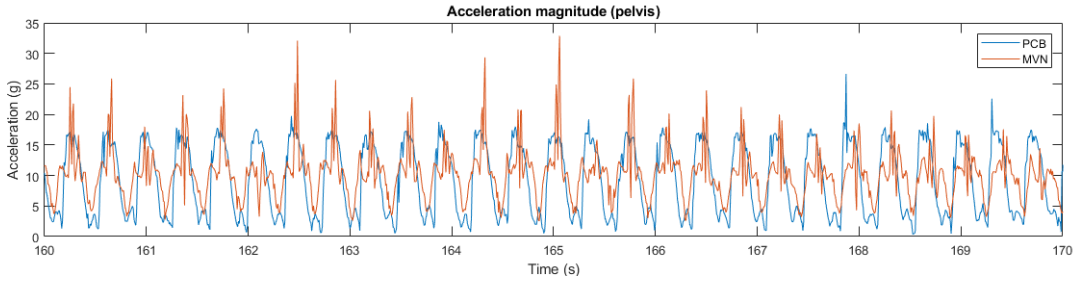

Figure 4.7: Magnitude of accelerations acquired with the Xsens MVN suit (red) and with the ICM-20648 sensors incorporated in the designed PCBs (blue). Depicted pelvis region.

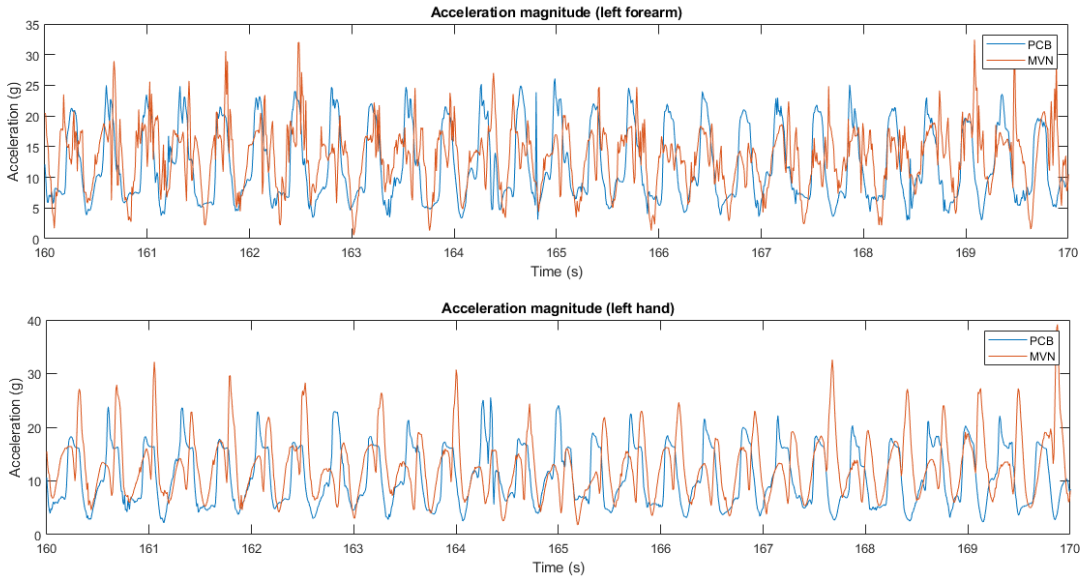

Figure 4.8: Magnitude of accelerations acquired with the Xsens MVN suit (red) and with the ICM-20648 sensors incorporated in the designed PCBs (blue). Depicted, from top to bottom, left forearm and left hand.

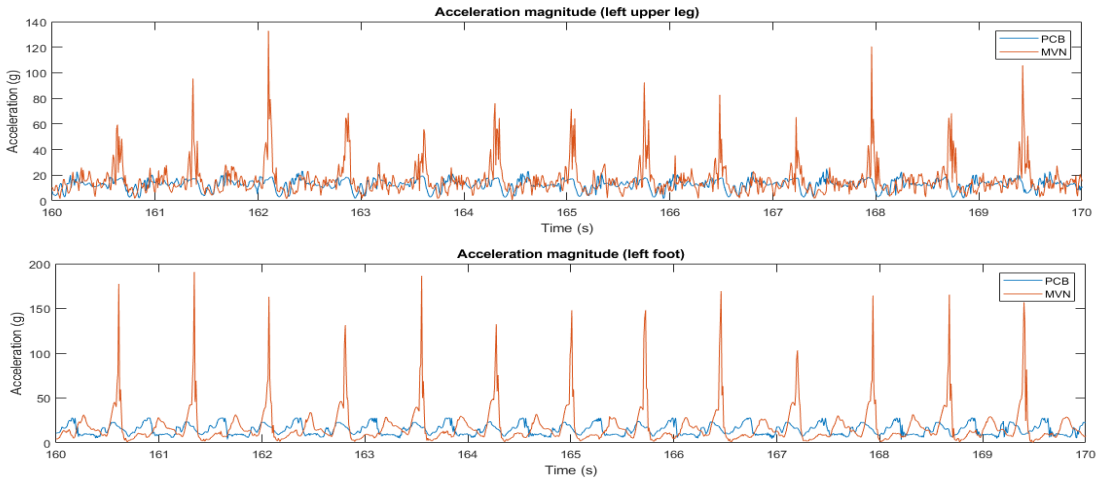

Figure 4.9: Magnitude of accelerations acquired with the Xsens MVN suit (red) and with the ICM-20648 sensors incorporated in the designed PCBs (blue). Depicted, from top to bottom, left upper leg and left foot.

To evaluate the correlation between the accelerometry data acquired with the two setups, the ICC coefficients were calculated for each body location. Accelerometry data from the Xsens MVN suit was considered as ground-truth. Data from the sensor boards was down-sampled to 120Hz, and the samples from both setups were subsequently normalized. The results are presented in table 4.1, leading to the conclusion that the designed sensor boards can be considered a viable and much cheaper alternative to the Xsens MVN suit.

Location	Pelvis	Left forearm	Left hand	Left upper leg	Left foot
ICC coefficient	0.747	0.688	0.726	0.426	0.418
$CI_{95\%}$	[0.714,0.777]	[0.453,0.822]	[0.594,0.815]	[0.112,0.709]	[0.096,0.689]

Table 4.1: ICC coefficients with a 95% Confidence Interval (CI) between the developed sensor boards and Xsens MVN suit signals, for each body part.

4.3 Software Implementation

The current section presents the software component of the developed prototype: the programming environment, the procedures adopted for data collection and processing, and for for energy expenditure computation.

4.3.1 Programming environment

In order to acquire data from the all the components of the prototype, a Python API for Linux was developed. This programming language was chosen to facilitate device synchronization

between *BITalino* devices [5] and the remaining components. To program the ESP32 microcontroller, the Arduino Software IDE was used. This platform supports C/C++ languages and was used to read data from the sensors on the smaller PCBs and send it to the computer. To acquire data from the Xsens MVN suit, the MVN Studio software was used. For data processing, MATLAB was the chosen platform. To implement and execute the code of the algorithms for energy expenditure computation, Google Collaboratory, an online platform that runs in a cloud and supports machine learning libraries, was used.

4.3.2 Data collection

For the data acquisition process, two personal computers (PCs) were used: one to acquire data from the *BodyEnergyExpenditure* prototype and one to acquire data from the Xsens MVN suit. The system clocks on both PCs were previously synchronized to carry out the acquisitions.

Heart rate, muscle oxygenation, 3D accelerations (from the designed sensor boards)[6] and skin EDA values were sent simultaneously to one PC. The synchronization between the data from all sensors was made by registering the timestamp at the start of the test, i.e. on the fifth minute of the experiment (see figure 3.7 of section 3.3.3). Heart rate and muscle oxygenation were sent via BLE, at 1Hz and 4Hz, respectively. 3D accelerations were sent via Bluetooth RFCOMM at 125Hz, and skin EDA was sent via Bluetooth 2.0 at 100Hz. For each participant, the values were stored into separated CSV files.

Data from the Xsens MVN suit was collected to the other PC using the MVN Studio software, an easy-to-use graphical user interface for real-time data recording. For each participant, 3D accelerations were recorded at 120Hz (maximum update rate of the suit) and stored into CSV files. The synchronization procedure was the same used with the energy meter prototype.

4.3.3 Data processing: PCB MEMS accelerometer calibration

MEMS accelerometers are sensors characterized by their high accuracy. Typically they are factory calibrated, but is recommended to calibrate the accelerometers to remove inaccuracies stemming from manufacturing imperfections, temperature variations, and installation issues

[5] The open-source code to acquire data from *BITalino* sensors is written in Python.

[6] 3D accelerations from the designed PCBs were only acquired in the experiments described in section 4.2.3.

[24]. Hence, a simple calibration procedure [63] was made for the MEMS accelerometers in the designed sensor boards and is described in appendix D.

4.3.4 Energy expenditure computation

To implement the multiple linear regression models for energy expenditure computation, the Google Colaboratory[7] platform was used. Google Colaboratory is a free online notebook environment that runs entirely in the cloud, containing all the necessary libraries for the development and execution of Python code, including machine learning algorithms.

The heart rate, accelerometry, muscle oxygenation, and EDA data of the twenty participants was processed, as described in section 3.3.3, and combined into a single CSV file. This file was uploaded to the Google Collaboratory cloud and served as the dataset used for the computation of energy expenditure and other metrics (e.g., RMSE).

4.4 Energy meter testing

During the development of the prototype, several tests were made that allowed validating its functionalities by detecting errors and existing bugs. This section covers the unitary, integration, and system tests performed for the verification and validation of the developed embedded system (HW + SW) for energy expenditure estimation.

4.4.1 Unitary tests

During the development of the embedded system, unitary tests were carried out. The purpose of these tests was to verify the correct implementation of each unit of the system separately. As new components were implemented, they were tested with various configurations, in separate programs, with subsequent observation of the output.

For each module, the following unitary tests were carried out:

- sensor data acquisition;
- sensor data writing into files;
- connection establishment between PC and sensor/component;
- connection closing between PC and sensor/component.

[7] `https://colab.research.google.com/notebooks/intro.ipynb`

4.4.2 Integration tests

Integration tests aim to find integration failures among the units that incorporate the embedded system. For their implementation, the *bottom-up* strategy was used, which consists of testing each module individually, and subsequently adding new modules and layers until the final system is reached.

Initially, each component of the BITalino module was tested individually and in conjunction with the other BITalino components, but isolated from the other modules. Subsequently, the Polar H7 band, the Humon Hex, the developed PCBs, and the MVN suit modules were integrated. For each integration of a new module, the following tests were carried out:

- data acquisition from multiple sensors/components simultaneously;
- data writing from multiple sensors into files;
- connection establishment between PC(s) and multiple sensors/components;
- connection closing between PC(s) and multiple sensors/components.

4.4.3 System tests

The last tests carried out were the system tests, which aimed to ensure that the embedded system met the requirements initially defined and specified. Among the various types of system tests, performance tests were performed as follows:

- data acquisition from multiple sensors/components simultaneously during 20 minutes;
- data acquisition from multiple sensors/components simultaneously with different distances between sensors and PCs.

4.4.4 Summary

The final version of the developed prototype includes a set of low-cost sensors for the acquisition of signals from metrics related with energy expenditure. It was intended to incorporate an optimal number of sensors to allow its use anywhere and avoid restrictions to the individual's natural movements during the execution of the workout. The tests carried out for the prototype validation demonstrate that the proposed solution can be considered an acceptable alternative if one desires to measure energy expenditure associated to physical exercise.

5 Conclusions and future work

This dissertation aimed to develop and validate a prototype of a wearable energy expenditure meter for the human body, based on the use of different sensors and sensor fusion methods. The development was carried out in collaboration with Sports Science experts affiliated with FCDEF-UC.

The most reliable methods for measuring energy expenditure are expensive, require a laboratory environment to be used and specialists to interpret the results, which are not provided in real-time. For these reasons, they become hard and impractical to use in real-life situations. The developed prototype presents a cheaper and less intrusive alternative solution to measure energy expenditure, allowing its use inside and outside the laboratory environment. However, some limitations should be considered. First, due to the Covid-19 pandemic situation, it was not possible to validate the prototype based on the reference methods. Secondly, it was not possible to carry out validation tests for indoor cycling and CrossFit, only for running. Finally, it was also not possible to obtain the final version of the prototype in time for more extensive experiments to be carried out for its validation with a representative sample of individuals. Despite the difficulties experienced throughout the work, it is believed that the main objectives were achieved.

In the future, new types of physical exercise may be added, including team sports. There are also features that can be added to the developed prototype, namely the inclusion of new sensors, for instance, to measure lactate through sweat. Some hardware improvements can also be made. It is recommended to encapsulate the designed sensor boards and the BITalino units, not only to protect the components, but also to avoid injuries and discomfort to the subject. Finally, a possible complement to this work is the creation of a virtual reality system for motion capture and recording in real-time. This would allow coaches or specialists in individual sports to analyze the technical gestures performed by athletes and simultaneously know the associated energy cost.

References

[1] Bitalino - Plux store, October 2020. [Online]. Available: "https://plux.info/14-bitalino".

[2] FAQ - Humon, September 2020. [Online]. Available: "https://humon.es/en/faq/".

[3] Humon - The World's First Muscle Oxygen Sensor, September 2020. [Online]. Available: "https://humon.io/".

[4] Introduction to Bluetooth Low Energy: A basic overview of key concepts for BLE - GATT, May 2020. [Online]. Available: "https://learn.adafruit.com/introduction-to-bluetooth-low-energy/gatt".

[5] The practical guide to hacking Bluetooth Low Energy, May 2020. [Online]. Available: "https://blog.attify.com/the-practical-guide-to-hacking-bluetooth-low-energy/".

[6] Kimberly A., Ingraham, Daniel P. Ferris, and C. David Remy. Evaluating physiological signal salience for estimating metabolic energy cost from wearable sensors. *Journal of applied physiology*, 126(3):717–729, March 2019.

[7] Levine J. A. Non-exercise activity thermogenesis (NEAT). *Best Practice & Research: Clinical Endocrinology & Metabolism*, 16(4):679–702, 2002.

[8] Kimberly A. Ingraham ad Elliott J. Rouse and C. David Remy. Accelerating the estimation of metabolic cost using signals derivatives. *IEEE Robotics and Automation Magazine*, December 2019.

[9] Qingbo Ana, Shiyu Ganc, Jianan Xua, Yu Baoc, Tongshun Wuc, Huijun Konga, Lijie Zhongc, Yingming Mac, Zhongqian Songa, and Li Niua. A multichannel electrochemical all-solid-state wearable potentiometric sensor for real-time sweat ion monitoring. *Electrochemistry Communications*, 107, September 2019.

[10] Weir J. B. New methods for calculating metabolic rate with special reference to protein metabolism. *Journal of Physiology*, 109:1–9, August 1949.

[11] Aquarat's blog. Humon hex bluetooth protocol - reverse engineering the humon hex muscle oxygenation sensor's bluetooth protocol, September 2020. [Online]. Available: "`https://aquarat.co.za/2018/10/16/reverse-engineering-the-humon-hex-muscle-oxygenation-sensors-bluetooth-protocol/`".

[12] Carlijn V. Bouten, Klaas R. Westerterp, Maarten Verduin, and Jan D. Janssen. Assessment of energy expenditure for physical activity using a triaxial accelerometer. *Medicine and Science in Sports and Exercise*, April 1994.

[13] S. Brage, N. Brage, P. W. Franks, U. Ekelund, M. Y. Wong, L. B. Andersen, K. Froberg, and N. J. Wareham. Branched equation modeling of simultaneous accelerometry and heart rate monitoring improves estimate of directly measured physical activity energy expenditure. *Journal of applied physiology*, 96(1):343–351, September 2004.

[14] Tudor-Locke C. and Basset DR Jr. How many steps/day are enough? Preliminary pedometer indices for public health. *Sports Med*, 34(1):1–8, 2004.

[15] S. Carneiro, Joana Silva, Bruno Aguiar, Tiago Rocha, Inês Sousa, Tiago Montanha, and José Ribeiro. Accelerometer-based methods for energy expenditure using the smartphone. *2015 IEEE International Symposium on Medical Measurements and Applications (MeMeA) Proceedings*, pages 151–156, 2015.

[16] C. J. Caspersen, K. E. Powell, and G. M. Christenson. Physical activity, exercise, and physical fitness: definitions and distinctions for health-related research. *Public Health Reports*, 100(2):126–131, 1985.

[17] Mario Cifrek, Vladimir Medved, Stanko Tonkovic, and Sasa Ostojic. Surface EMG based muscle fatigue evaluation in biomechanics. *Clinical Biomechanicals*, 24(4):327–340, May 2009.

[18] Laurence A. Cole. *Biology of Life*, USA 2016.

[19] Hugo D. Critchley. Review: Electrodermal responses: What happens in the brain. *The Neuroscientist*, 8(2):132–142, April 2002.

[20] Schoeller DA and van Santen E. Measurement of energy expenditure in humans by doubly labeled water method. *J Appl Physiol*, 53(4):955–959, 1982.

[21] Pietro Enrico di Prampero and Cristian Osgnach. Metabolic power in team sports - part 1: An update. *International Journal of Sports Medicine*, 39(8):581–587, July 2018.

[22] Ainsworth B. E., Haskell W. L., Herrmann S. D., Meckes N., Bassett D. R. Jr, Tudor-Locke C., Greer J. L., Vezina J., Whitt-Glover M. C., and Leon A. 2011 Compendium of physical activities: a second update of codes and MET values. *Medicine & Science in Sports & Exercise*, 43:1575–1581, 2011.

[23] Melanson EL, Knoll JR, Bell ML, Donahoo WT, Hill JO, Nysse LJ, and et al. Commercial available pedometers: considerations for accurate step counting. *Prev Med*, 39(2):361–368, 2004.

[24] Digikey Eletronics. A designer's guide to MEMS sensors, May 2020. [Online]. Available: "`https://www.digikey.com/en/articles/a-designers-guide-to-mems-sensors`".

[25] Katherine Ellis, Jacqueline Kerr, Suneeta Godbole, Gert Lanckriet, David Wing, and Simon Marshall. A random forest classifier for the prediction of energy expenditure and type of physical activity from wrist and hip accelerometers. *Physiological Measurement*, 35:2191–2203, October 2014.

[26] Miikka Ermes, Juha Parkka, Jani Mantyjarvi, and Ilkka Korhonen. Detection of daily activities and sports with wearable sensors in controlled and uncontrolled conditions. *American College of Sports Medicine*, 12(1):20–26, January 2008.

[27] Espressif Systems. *ESP32 Series Datasheet*, 2019. V3.0.

[28] FACRDr. Crossfit: Now get the perfectly sculpted body with this explosive gym routine, April 2020. [Online]. Available: "`https://factdr.com/fitness-and-exercise/fitness/crossfit/`".

[29] Dusan Fiala, George Havenith, Peter Bröde, Bernhard Kampmann, and Gerd Jendritzky. UTCI-Fiala multi-node model of human heat transfer and temperature regulation. *International Journal of Biometeorology*, 56:429–441, November 2012.

[30] Dusan Fiala, Keviv J. Lomas, and Martin Stohrer. A computer model of human thermoregulation for a wide range of environmental conditions: the passive system. *Journal of applied physiology*, 87(5):1957–1972, November 1999.

[31] Marc D. Gellman and J. Rick Turner. *Encyclopedia of Behavioral Medicine*. Springer-Verlag, New York, 2013.

[32] Hristijan Gjoreski, Bostjan Kaluza, Matjaz Gams, Radoje Milic, and Mitja Lustrek. Context-based ensemble method for human energy expenditure estimation. *Applied Soft Computing*, 37:960–970, May 2015.

[33] Miriam González-Izal, Armando Malanda, Esteban Gorostiaga, and Mikel Izquierdo. Electromyographic models to assess muscle fatigue. *Journal of Electromyography and Kinesiology*, 22(4):501–512, August 2012.

[34] Tanaka H., Monahan K. D., and Seals D. R. Aging-predicted maximal heart rate revisited. *Journal of the American College of Cardiology*, 37:153–156, 2001.

[35] W. L. Haskell, M. C. Yee, A. Evans, and P. J. Irby. Simultaneous measurement of heart rate and body motion to quantitate physical activity. *Medicine & Science in Sports & Exercise*, 25(1):109–115, January 1993.

[36] Heather A. Haugen, Lingtak-Neander Chan, and Fanny Li. Indirect calorimetry: a practical guide for clinicians. *Nutr Clin Pract*, 22(4):377–388, August 2007.

[37] Wenya He, Chunya Wang, Huimin Wang, Muqiang Jian, Wangdong Lu, Xiaoping Liang, Xin Zhang, Fengchun Yang, and Yingying Zhang. Integrated textile sensor patch for real-time and multiplex sweat analysis. *Science Advances*, 5(11), November 2019.

[38] Andrew Hills, Najat Mokhtar, and Nuala M. Byrne. Assessment of physical activity and energy expenditure: an overview of objective measures. *Frontiers in Nutrition*, 1(5), June 2014.

[39] Arizona State University & National Cancer Institute. Compendium of Physical Activities, June 2020. [Online]. Available: "`https://sites.google.com/site/compendiumofphysicalactivities/`".

[40] Boot Camp & Military Fitness Institute. Factors affecting energy expenditure, March 2020. [Online]. Available: "`https://bootcampmilitaryfitnessinstitute.com/anatomy-physiology/factors-affecting-energy-expenditure/`".

[41] Achten J and Jeukendrup AE. Heart rate monitoring: applications and limitations. *Sports Med*, 33(7):517–538, 2003.

[42] Andrew M. Jones and Jonathan H. Doust. A 1% treadmill grade most accurately reflects the energetic cost of outdoor running. *Journal of Sports Sciences*, 14(4):321–327, January 1996.

[43] Snellen JW, Chang KS, and Smith W. Technical description and performance characteristics of a human whole-body calorimeter. *Med Biol Eng Comput*, 21:9–20, 1983.

[44] LR Keytel, JH Goedecke, TD Noakes, H. Hiiloskorpi, R Laukkanen, L van der Merwe, and EV Lambert. Prediction of energy expenditure from heart rate monitoring during submaximal exercise. *Journal of Sports Sciences*, 23(3):289–97, April 2005.

[45] Karsten Koehler and Clemens Drenowatz. Monitoring energy expenditure using a multi-sensor device - applications and limitations of the sensewear armband in athletic populations. *Frontiers in Physiology*, 8(983), Nov 2017.

[46] Lin, Che-wei, Ya ting C. Yang, Jeen shing Wang, and Yi ching Yang. A wearable sensor module with a neural-network- based activity classification algorithm for daily energy expenditure estimation. *IEEE Transactions on Information Technology in Biomedicine*, 16(5):991–998, September 2012.

[47] Shaopeng Liu, Robert X. Gao, and Patty S. Freedson. Computational methods for estimating energy expenditure in human physical activities. *American College of Sports Medicine*, 44(11):2138–2146, May 2012.

[48] Firstbeat Technologies Ltd. An energy expenditure estimation method based on heart rate measurement. March 2012.

[49] Firstbeat Technologies Ltd. Automated fitness level (VO2max) estimation with heart rate and speed data. November 2014.

[50] M. J. Mathie, B. G. Celler, N. H. Lovell, and A. C. F. Coster. Classification of basic daily movements using a triaxal accelerometer. *Medical and Biological Engineering and Computing*, 42:679–687, 2004.

[51] William D. McArdle, Frank I. Katch, and Victor L. Katch. *Exercise Physiology: Nutrition, Energy, and Human Performance*. Lippincott Williams & Wilkins, 2007.

[52] Gregoire P. Millet, V.E. Vleck, and D.J. Bentley. Physiological differences between cycling and running - lessons from triathletes. *Sports Medicine*, 39(3):179–206, February 2009.

[53] Sakchai Muangsrinoon and Poonpong Boonbrahm. Burn in zone: Real time heart rate monitoring for physical activity. *International Joint Conference on Computer Science and Software Engineering*, pages 1–6, 2017.

[54] Didace Ndahimana and Eun-Kyung Kim. Measurement methods for physical activity and energy expenditure: a review. *Clinical Nutrition Research*, 6:68–80, April 2017.

[55] American College of Sports Medicine. ACSM's guidelines for exercise testing, April 2020. [Online]. Available: "`https://www.acsm.org/docs/default-source/publications-files/acsm-guidelines-download-10th-edabf32a97415a400e9b3be594a6cd7fbf.pdf?sfvrsn=aaa6d2b2_0`".

[56] Harsh Patel, Hassan Alkhawam, Raef Madanieh, Niel Shah, Constantine E. Kosmas, and Timothy J. Vittorio. Aerobic vs anaerobic exercise training effects on the cardiovascular system. *World Journal of Cardiology*, 9(2):134–138, 2017.

[57] Harry H. Pennes. Analysis of tissue and arterial blood temperatures in the resting human forearm. *Journal of applied physiology*, 1(2):93–121, August 1948.

[58] Eric T. Poehlman. A review: exercise and its influence on resting energy metabolism in man. *Medicine & Science in Sports & Exercise*, 21(5):515–525, 1989.

[59] Hugo F. Posada-Quintero, Natasa Reljin, Craig Mills, Ian Mills, John P. Florian, Jaci L. VanHeest, and Ki H. Cho. Time-varying analysis of electrodermal activity during exercise. *Nutr Clin Pract*, 13(6), 2018.

[60] Luís Rama. *Teoria e Metodologia do Treino - Modalidades Individuais*. Instituto Português do Desporto e Juventude, 2016.

[61] Kirsten L. Rennie, Susie J. Hennings, Jo Mitchell, , and Nicholas J. Wareham. Estimating energy expenditure by heart-rate monitoring without individual calibration. *Medicine & Science in Sports & Exercise*, 33(6):939–945, July 2000.

[62] Eliane Lopes Rosado, Vanessa Chaia Kaipper, and Roberta Santiago de Brito. Energy expenditure measured by indirect calorimetry in obesity. *Applications of Calorimetry in a Wide Context – Differential Scanning Calorimetry, Isothermal Titration Calorimetry and Microcalorimetry*, January 2013.

[63] STMicroeletronics. Using LSM303DLH for a tilt compensated electronic compass. pages 1–34, August 2010.

[64] TDK InvenSense. *6-Axis MEMS MotionTracking™ Device with Enhanced EIS Support and Sensor Fusion Processing*, October 2017. Rev. 1.2.

[65] Texas Instruments. *TCA9548A Lo2-Voltage 8-Channel I2C Switch with Reset*, November 2019. Rev. G.

[66] A. C. Pinheiro Volp, F. C. Esteves de Oliveira, R. Duarte Moreira Alves, E. A. Esteves, and J. Bressan. Energy expenditure: components and evaluation methods. *Nutrición Hospitalaria*, 26(3):430–440, 2011.

[67] Daniel Wendt, Luc J. C. van Loon, and Wouter D. van Marken Lichtenbelt. Thermoregulation during exercise in the heat - strategies for maintaining health and performance. *Sports Medicine*, 37(8):669–682, 2007.

[68] Leonard WR. Laboratory and field methods for measuring energy expenditure. *Am J Hum Biol*, 24(3):372–384, 2012.

[69] Che-Chang Yang and Yeh-Liang Hsu. A review of accelerometry-based wearable motion detectors for physical activity monitoring. *Sensors*, 10(8):7772–7788, August 2010.

[70] Lam YY, Redmand LM, Smith SR, Bray GA, Greenway FL, Johannsen D, and et al. Determinants of sedentary 24-h energy expenditure: equations for energy prescription and adjustments in a respiratory chamber. *Am J Clin Nutr*, 99:834–842, 2014.

Appendix A

Schematic and board diagrams

Figure A.1 shows the schematic diagram of the designed PCB for the primary board of the prototype, including the operating circuit of each module and the connections between them.

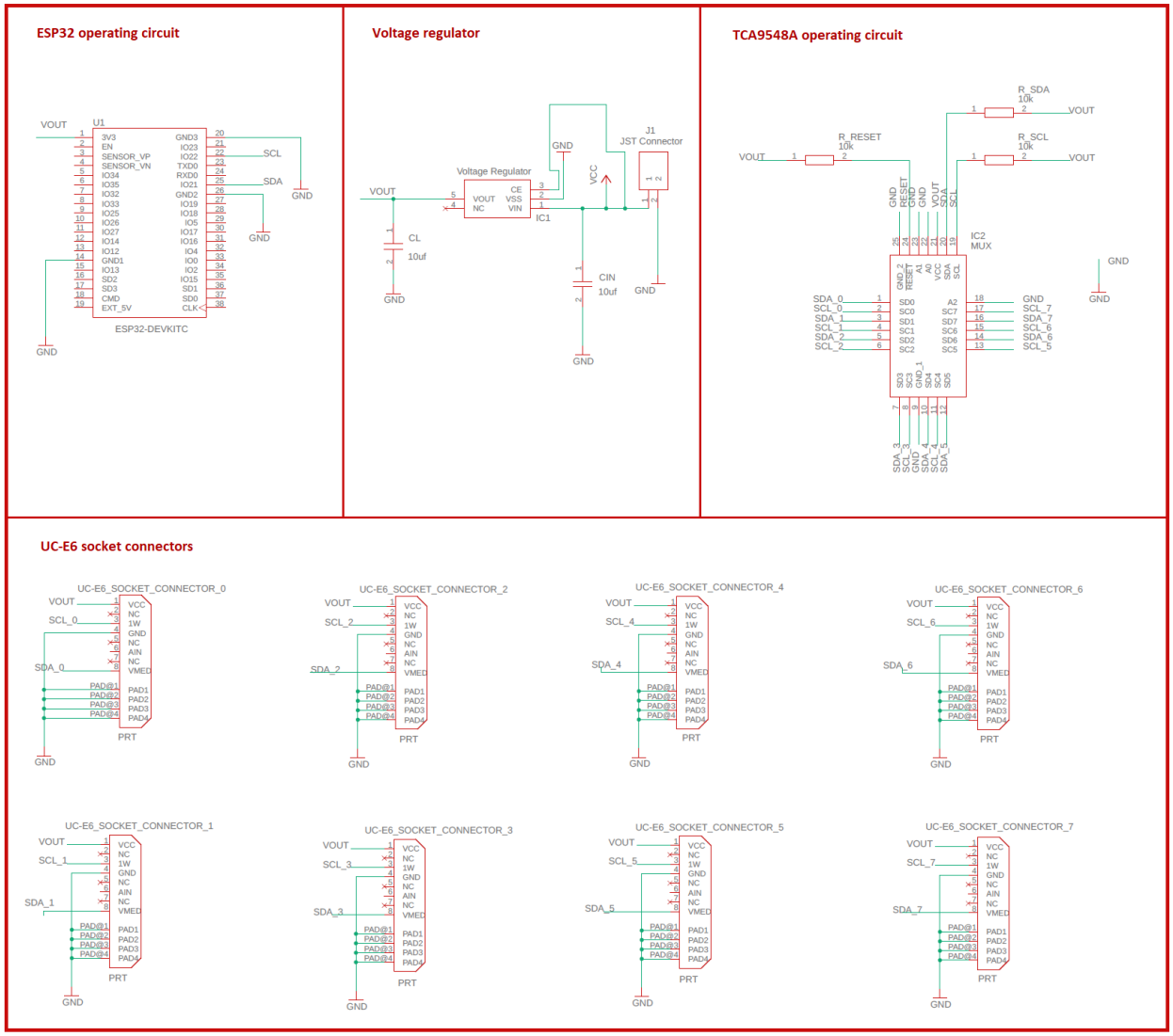

Figure A.1: Main board schematic diagram.

In figure A.2 is illustrated the PCB design of the primary board. Figure A.2a shows all the connections on both layers without the ground plane layout (dimensions in millimeters). Figure A.2b illustrates the top layer with the ground plane layout included. Figure A.2c illustrates the bottom layer with the ground plane layout included.

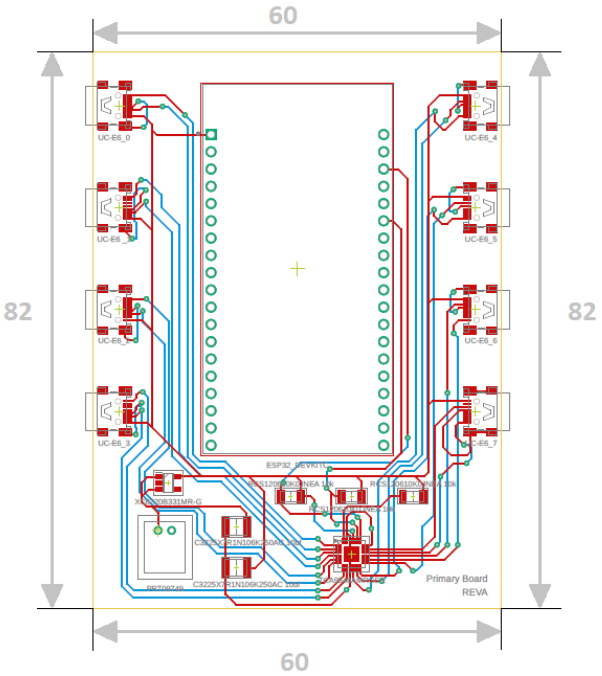

(a) Primary board layout.

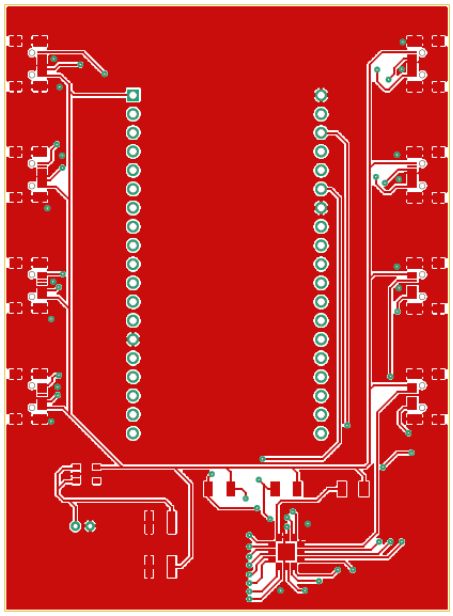

(b) Top layer.

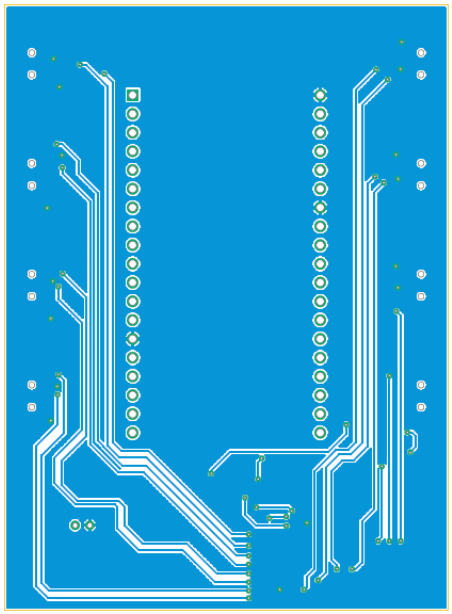

(c) Bottom layer.

Figure A.2: Primary board PCB design.

Figure A.3 shows the schematic diagram of the designed PCB for the smaller board of the prototype.

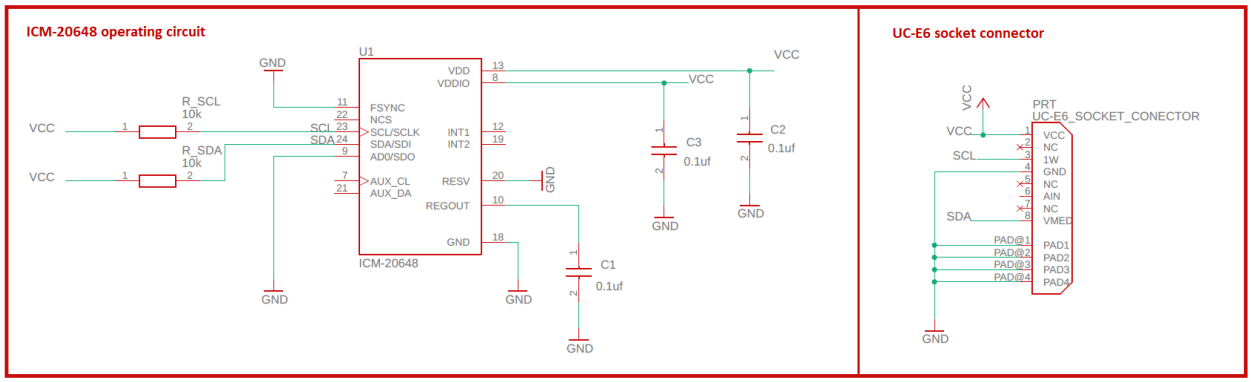

Figure A.3: Smaller board schematic diagram.

In figure A.4 is illustrated the PCB design of the smaller board. Figure A.4a shows all the connections on both layers without the ground plane layout (dimensions in millimeters). Figure A.4b illustrates the top layer with the ground plane layout included. Figure A.4c illustrates the bottom layer with the ground plane layout included.

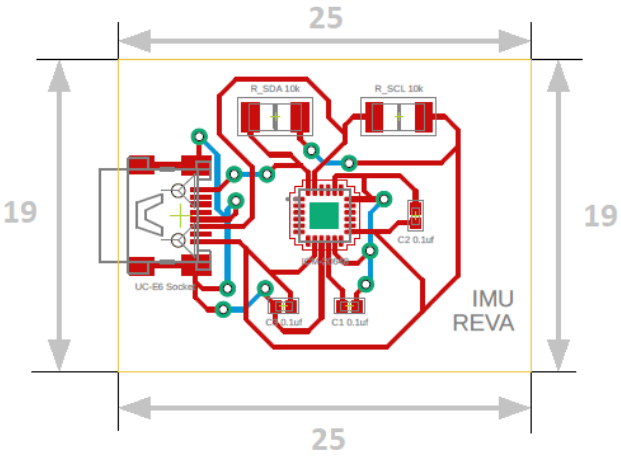

(a) Small board layout.

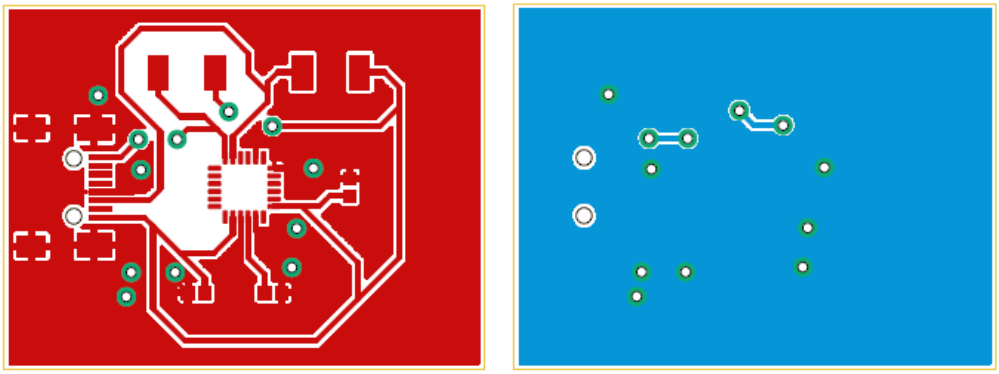

(b) Top layer.

(c) Bottom layer.

Figure A.4: Small board PCB design.

Appendix B

UTCI-Fiala model of human heat transfer and temperature regulation

This appendix provides a general overview of the Universal Thermal Climate Index (UTCI) Fiala model for heat transfer and temperature regulation, summarizing the algorithms published by Dusan Fiala, et al. [29].

B.1 Body construction

The UTCI-Fiala model consists of 12 spherical or cylindrical body setions: head, face, neck, shoulders, thorax, abdomen, upper and lower arms, hands, upper and lower legs, and feet (Figure B.1).

Body elements are built of annular concentric tissue layers (section A-A" in Figure B.1): brain, lung, bones, muscles, viscera, fat, and skin and are subdivided into a total of 63 spatial sectors (Figure B.2).

The model represents an average person with a body surface area of $1.85m^2$, body weight of 73.4kg, body fat content of 14%, basal metabolism of 87.1 W, basal evaporation rate from the skin of 18W, cardiac output of $4.9L.min^{-1}$, skin blood flow of $0.4L.min^{-1}$, and skin wetness of 6%.

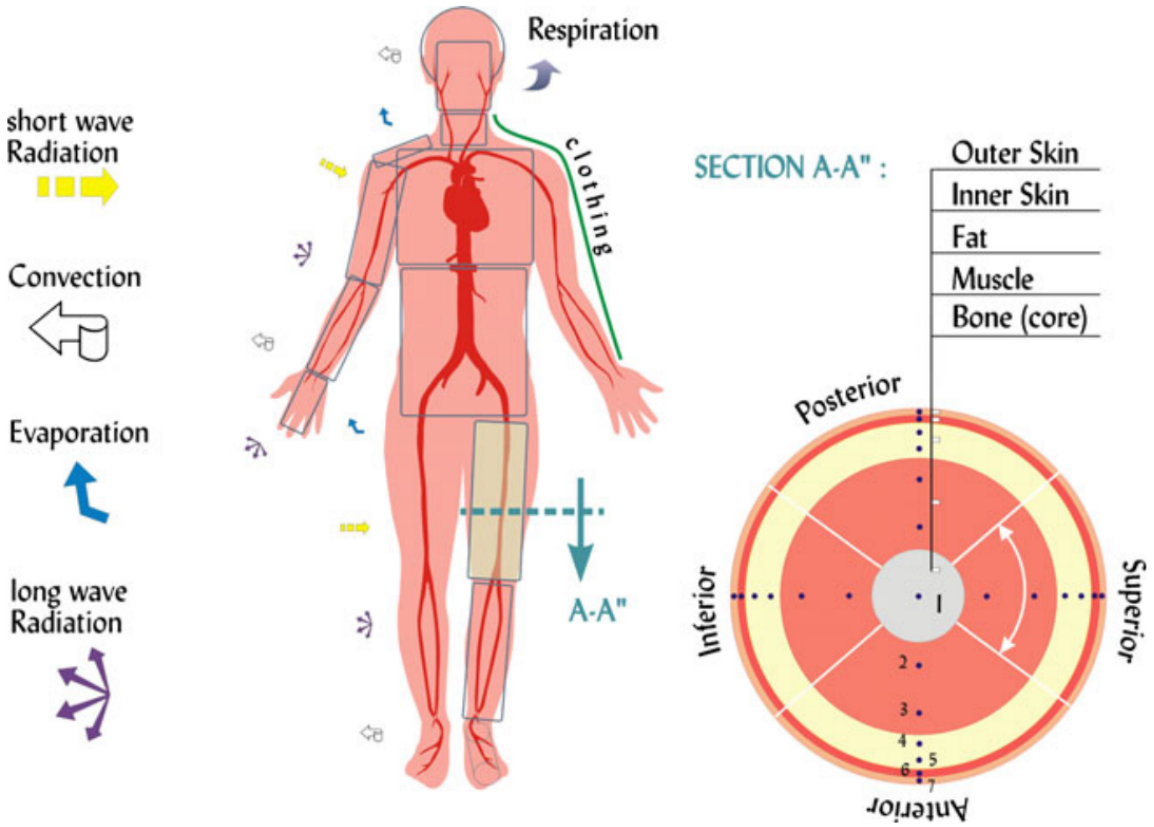

Figure B.1: Schematic diagram of the UTCI-Fiala model (reproduced from [29]).

Body element	Length (m)	Outer radius (m)	Central angle (deg)	Surface area (m^2)	Spatial sectors - angle (deg)			
					Anterior	Posterior	Inferior	Superior
Head		0.1040	180.0	0.068	16.0	164.0		
Face	0.0984	0.0780	210.0	0.028	98.0			112.0
Neck	0.0842	0.0567	360.0	0.030	58.0	80.0		222.0
Shoulders	0.3200	0.0460	130.0	0.033				130.0
Thorax	0.3060	0.1290	360.0	0.248	165.0	149.0	46.0	
Abdomen	0.5520	0.1260	360.0	0.230	133.0	131.0	96.0	
Upper arms	0.6380	0.0430	360.0	0.172	77.0	76.0	52.0	155.0
Lower arms	0.6360	0.0404	360.0	0.161	44.0	59.0	128.0	129.0
Hands	0.6200	0.0226	360.0	0.088			183.0	177.0
Upper legs	0.7020	0.0584	360.0	0.258	95.0	79.0	83.0	103.0
Lower legs	0.6880	0.0511	360.0	0.221	68.0	99.0	89.0	104.0
Feet	0.4800	0.0350	360.0	0.106	239.0	121.0		

Figure B.2: Body geometry parameters.

B.2 Heat exchanges within the tissues

The mechanisms of heat and mass transport within the tissues of the human organism are modeled using the Bio-Heat Transfer Equation of Pennes [57]. This differential equation

describes the heat dissipation in a homogeneous, infinite tissue volume and is given by:

$$k(\frac{\partial^2 T}{\partial r^2} + \frac{\omega}{r}\frac{\partial T}{\partial r}) + q_m + \rho_{bl} w_{bl} c_{bl}(T_{bl,a} - T) = \rho c \frac{\partial T}{\partial t}. \tag{B.1}$$

From left to right, the first term corresponds to the heat-conduction term, i.e., the radial heat flow from warmer to colder tissue regions, where k is the thermal conductivity ($W.m^{-1}.K^{-1}$), T is the tissue temperature ($^{\circ}C$), r is the radius (m) and ω is a geometry factor :$\omega = 1$ for polar coordinates (e.g., leg) and $\omega = 2$ for spherical coordinates (e.g., head). The second term expresses the metabolic heat production, in W/m^3, and is given by the sum of the basal value, i.e. the energy needed to maintain processes essential for life during rest, and the additional heat that is produced during exercise and/or shivering. The third term represents the heat-convection term, the blood perfusion, where ρ_{bl} is the density of blood (kg/m^3), w_{bl} is the blood perfusion rate (s^{-1}), c_{bl} is the heat capacitance of blood ($J \cdot kg^{-1} \cdot K^{-1}$), and $T_{bl,a}$ is the arterial blood temperature ($^{\circ}C$). The right side of the equation corresponds to the storage of heat within the tissue mass, where ρ is the tissue density (kg/m^3), c is the tissue heat capacitance ($J.kg^{-1}.K^{-1}$) and t is the time (s) [30].

B.3 Heat exchange with the environment: boundary conditions

The metabolic heat that reaches the skin is lost to the environment in different ways including convection, radiation, and evaporation. The rate of heat exchange varies over the body and can also be affected by the clothes worn.

The heat flux q_{sk}, passing the surface of a peripheral sector of skin is equivalent to:

$$q_{sk} = q_{cnv} + q_{rlw} - q_{rsw} + q_{evp} \tag{B.2}$$

- q_{sk} - heat flux passing the surface of a peripheral sector of skin given in W/m^2;
- q_{cnv} - heat exchanged by convection with the ambient air given in W/m^2;
- q_{rlw} - heat exchange by radiation with surrounding surfaces given in W/m^2;
- q_{rsw} - heat exchanged by irradiation from high-temperature sources given in W/m^2;
- q_{evp} - heat exchanged by evaporation of moisture from the skin given in W/m^2.

B.3.1 Convection

The convective heat exchange $q_{cnv}(W.m^{-2})$ between a body sector of surface temperature T_{bs}(K) and ambient air of temperature T_a(K) is given by:

$$q_{cnv} = h_{c,mix}(T_{bs} - T_a) \tag{B.3}$$

The convection coefficients, $h_{c,mix}$ $(W.m^{-2}.K^{-1})$, are calculated based on the location at the body (B.3), the temperature difference between the body surface, T_{bs} (K), and the air, T_a (K), and the local air speed, v_a (m/s):

$$h_{c,mix} = \sqrt{a_{Nat}\sqrt{T_{bs} - T_a} + a_{For}.v_a + a_{Mix}} \tag{B.4}$$

Body element	Mixed convection heat transfer coefficient $h_{c,mix}$ (W $m^{-2}K^{-1}$)			Surface absorptivity α_{bs}	View factors (standing posture) between body sector and the environment $\phi_{bs\text{-}env}$			
	a_{Nat}	a_{For}	a_{Mix}		Anterior	Posterior	Inferior	Superior
Head	3.000	113.00	−5.650	0.80	0.9869	0.9643		
Face	3.000	113.00	−5.650	0.99	0.8417	0.8909		
Neck	1.600	130.00	−6.500	0.99	0.7792	0.9433	0.8569	
Shoulders	5.900	216.00	−10.800	0.99	0.9048			
Thorax	0.500	180.00	−7.400	0.99	0.9314	0.9590	0.4408	
Abdomen	1.200	180.00	−9.000	0.99	0.8923	0.8886	0.6323	
Upper arms	8.270	216.02	−10.801	0.99	0.7546	0.9268	0.3356	0.9821
Lower arms	8.270	216.02	−10.801	0.99	0.8774	0.9639	0.5065	0.9967
Hands	8.270	216.02	−10.801	0.99	0.8835	0.3801		
Upper legs	5.300	220.00	−11.000	0.99	0.8761	0.9374	0.4693	0.8793
Lower legs	5.300	220.00	−11.000	0.99	0.9282	0.9393	0.7264	0.9800
Feet	6.800	210.00	−10.500	0.99	0.8602	0.8955		

Figure B.3: Environmental heat exchange parameters.

B.3.2 Radiation

To calculate the long-wave portion of the radiative heat exchange (q_{rlw}), the model employs the concept of (directional) mean surface temperatures of the radiant envelope that encloses a body sector using the corresponding sector's view factor:

$$q_{rlw} = \sigma\epsilon_{bs}\epsilon_{env}\phi_{bs-env}[(T_{abs} + 273)^4 - (T_{env} + 273)^4] \tag{B.5}$$

where $\sigma = 5.67.10^{-8}\ W.m^{-2}K^{-4}$ is the Stefan-Bolzmann constant, ϵ_{bs} and ϵ_{env} are the surface emissivity of the body sector ($\epsilon_{bs} = 0.95$ for UTCI clothing) and the radiant envelope (ϵ_{env}

= 1.0 for UTCI envelopes), respectively. T_{bs} and T_{env} are the surface temperatures of the body sector and the environment given in $°C$, respectively. The view factors ϕ_{bs-env} vary according to the location at the body and can be consulted in Figure B.3.

B.3.3 Irradiation

The irradiation of the body by high-temperature sources (sun, fireplaces, etc.) was also considered in formula B.2. The short-wave radiation absorbed by a sector surface is given by:

$$q_{rsw} = \alpha_{bs} f_s I_s \tag{B.6}$$

- q_{rsw} - short-wave radiation given in $W.m^{-2}$;
- α_{bs} - body surface short-wave absorptivity (depends on the color of the skin or the color of the covering material);
- f_s - body sector's projected area factor (depends on body posture and solar altitude);
- I_s - incident short-wave radiation given in $W.m^{-2}$.

B.3.4 Evaporation

Evaporation can be defined as the process of losing heat through the conversion of water to gas. The heat exchanged by evaporation of moisture from a skin sector of area A_{sk} is given by:

$$q_{evp} = \lambda_{H2O} \frac{dm_{sw}}{A_{sk} dt} + \frac{P_{osk,sat} - P_{sk}}{R_{e,sk}} \tag{B.7}$$

- q_{evp} - heat exchanged by evaporation of moisture from the skin given in $W.m^{-2}$;
- λ_{H2O} - vaporization heat of the water, $\approx 2256\ kJ.kg^{-1}$;
- A_{sk} - skin sector area given in m^2;
- $\frac{dm_{sw}}{dt}$ - rate of sweat production over A_{sk};
- $P_{osk,sat}$ - saturated vapour pressure within the outer skin given in Pa;
- P_{sk} - water vapor pressure at the skin surface, given in Pa;
- $\frac{1}{R_{e,sk}}$ - skin moisture permeability, $\approx 0.003\ W.m^{-2}.Pa^{-1}$.

For purposes of temperature regulation, evaporation heat losses through the skin of the human body can occur by sweat (first term of equation B.7) and moisture diffusion processes (second term of equation B.7). Studies have demonstrated that, for every mL of water that evaporates from the body surface, approximately 2.43 kJ of heat is lost and sweating rates of up to 3.5 L/hour have been reported in trained athletes [67]. Values of sweat rates can vary according to the type of exercise, environmental conditions and dehydration levels.

B.4 Heat exchanges with the environment: respiration

Although most of the heat is lost through the body surface, there is also a part that is lost by respiration. The total respiratory heat loss is given by the sum of the latent heat exchange of respiration, E_{rsp} (equation B.8), with the dry heat loss of respiration, C_{rsp} (equation B.9). Both terms are calculated from the pulmonary ventilation as a function of the whole body metabolism, i.e., $\int q_m dV$ (W):

$$E_{rsp} = 3.233 \int q_m dV (0.0277 - 6.5 \times 10^{-5} T_a - 4.91 \times 10^{-6} p_a) \tag{B.8}$$

$$C_{rsp} = 1.44 \times 10^{-3} \int q_m dV (32.6 - 0.934 T_a - 1.96 \times 10^{-4} p_a) \tag{B.9}$$

- E_{rsp} - latent heat exchange of respiration given in W;
- C_{rsp} - dry heat loss of respiration given in W;
- $\int$ q_m dV - pulmonary ventilation rate given in W;
- T_a - ambient air temperature given in $°C$;
- p_a - ambient air pressure given in Pa.

The total respiratory heat loss E_{rsp} + C_{rsp} is distributed over body elements of the pulmonary tract: face, neck and lungs.

Appendix C

Mathematical Background

C.1 Multiple Linear Regression Models

Multiple linear regression models were selected for the estimation of energy expenditure in the three physical exercises mentioned in section 3.1. For each multiple linear regression analysis, the signals were divided into two categories: physiological data and accelerometry data. Table C.1 summarizes the signals included in the two categories.

Category	**Signals**
Physiological data	Heart rate Muscle oxygenation Electrodermal activity Blood oxygenation
Accelerometry data	Magnitude of accelerations from multiple body locations, including pelvis, thoracic back, neck, head, shoulders, arms, forearms, hands, upper legs, lower legs, and feet.

Table C.1: Signal categories.

For each physical exercise, three models are proposed: one model containing physiological data; one model containing accelerometry data, and one model containing containing physiological and accelerometry data combined. The features of the proposed models for running, indoor cycling, and CrossFit are presented in table C.2.

Physical Exercise	Model	Signals
Running	Physiological data	Heart rate Muscle oxygenation Electrodermal activity
	Accelerometry data	Magnitude accelerations
	Combined data	Heart rate Muscle oxygenation Electrodermal activity Magnitude accelerations
Indoor cycling	Physiological data	Heart rate Muscle oxygenation Electrodermal activity Blood oxygenation
	Accelerometry data	Magnitude accelerations
	Combined data	Heart rate Muscle oxygenation Electrodermal activity Blood oxygenation Magnitude accelerations
CrossFit	Physiological data	Heart rate Blood oxygenation
	Accelerometry data	Magnitude accelerations
	Combined data	Heart rate Muscle oxygenation Magnitude accelerations

Table C.2: Proposed models for each of the 3 physical exercises: running, indoor cycling, and CrossFit.

At the time of this work, it was only possible to develop models for running. For this exercise, the energy expenditure can be estimated by one of the 3 following models:

Physiological data

$$EE = 0.1524 \times HR + 0.052 \times SMO2 - 11.5339 \times EDA + 13.7666. \quad \text{(C.1)}$$

- EE: energy expenditure, in kcal/min;
- HR: heart rate, in beats per minute;
- $SMO2$: muscle oxygenation, in percentage;
- EDA: electrodermal activity, in Siemens.

Accelerometry data

$$EE = 1.8872 \times A_{pelvis} - 0.4382 \times A_{lower\ back} + 9.7311 \times A_{medium\ back} - 3.8557 \times A_{upper\ back} + \\ + 1.1738 \times A_{neck} + 0.0798 \times A_{head} - 0.2261 \times A_{right\ shoulder} + 0.4126 \times A_{right\ upper\ arm} - \\ 0.0674 \times A_{right\ forearm} - 0.0727 \times A_{right\ hand} + 0.8251 \times A_{left\ shoulder} - 0.2934 \times A_{left\ upper\ arm} - \\ - 0.1946 \times A_{left\ forearm} - 0.2345 \times A_{left\ hand} + 0.0695 \times A_{right\ upper\ leg} - 0.0041 \times A_{right\ lower\ leg} + \\ + 0.0903 \times A_{right\ foot} + 0.0903 \times A_{right\ toe} + 0.0614 \times A_{left\ upper\ leg} + 0.0823 \times A_{left\ lower\ leg} + \\ + 0.0003 \times A_{left\ foot} - 0.0003 \times A_{left\ toe} - 8.6452 \times A_{lower\ thoracic\ back} + 2.1121. \quad \text{(C.2)}$$

- EE: energy expenditure, in kcal/min;
- A_l: Magnitude acceleration from body location l.

Combined data

$$EE = 0.1429 \times HR + 0.038 \times SMO2 - 7.4732 \times EDA + 1.7811 \times A_{pelvis} - 5.3313 \times A_{lower\ back} + \\ + 4.0916 \times A_{medium\ back} - 1.0710 \times A_{upper\ back} + 0.4060 \times A_{neck} + 0.0666 \times A_{head} - \\ - 0.2128 \times A_{right\ shoulder} - 0.1079 \times A_{right\ upper\ arm} - 0.0592 \times A_{right\ forearm} - 0.0633 \times A_{right\ hand} + \\ + 0.4887 \times A_{left\ shoulder} - 0.0862 \times A_{left\ upper\ arm} - 0.0748 \times A_{left\ forearm} - 0.0658 \times A_{left\ hand} + \\ + 0.0311 \times A_{right\ upper\ leg} - 0.0137 \times A_{right\ lower\ leg} - 0.0024 \times A_{right\ foot} - 0.0024 \times A_{right\ toe} + \\ - 0.0407 \times A_{left\ upper\ leg} + 0.0722 \times A_{left\ lower\ leg} + 0.0452 \times A_{left\ foot} - 0.0452 \times A_{left\ toe} - \\ - 5.8942 \times A_{lower\ thoracic\ back} - 11.6983. \quad \text{(C.3)}$$

- EE: energy expenditure, in kcal/min;
- HR: heart rate, in beats per minute;
- $SMO2$: muscle oxygenation, in percentage;
- EDA: electrodermal activity, in Siemens.

- A_l: Magnitude acceleration from body location l.

C.2 Pearson's Correlation Coefficient

The Pearson's correlation coefficient is a metric that measures the linear relationship between two variables, ranging from -1 to 1. The value of -1 expresses a linear negative correlation between the two variables, the value of 1 expresses a positive linear correlation, and the value of 0 means that there is no linear correlation between the two variables.

The Pearson's correlation coefficient ρ is calculated as:

$$\rho = \frac{\sum_{i=1}^{N}(x_i - \bar{x})(y_i - \bar{y})}{\sqrt{\sum_{i=1}^{N}(x_i - \bar{x})^2}.\sqrt{\sum_{i=1}^{N}(y_i - \bar{y})^2}}, \tag{C.4}$$

where x_1,x_2,...,x_N and y_1,y_2,...,y_N are the values from both variables, and $\bar{x}$ and $\bar{y}$ are the means of both variables expressed as:

$$\bar{x} = \frac{1}{N}\sum_{i=1}^{N} x_i, \tag{C.5}$$

and

$$\bar{y} = \frac{1}{N}\sum_{i=1}^{N} y_i. \tag{C.6}$$

C.3 ICC Coefficient Calculation

The intraclass correlation coefficient (ICC) is a parameter that measures the correlation between two or more measurement samples of a quantitative variable. ICC values range from 0 to 1, where a ICC value closer to 1 indicates high similarity between values, while a ICC value closer to 0 indicates low similarity between values.

Considering a dataset of N paired data values ($x_{n,1}$,$x_{n,2}$), for n = 1,...,i, the intraclass correlation r is expressed as:

$$r = \frac{1}{Ns^2}\sum_{i=1}^{N}(x_{i,1} - \bar{x})(x_{i,2} - \bar{x}), \tag{C.7}$$

where

$$\bar{x} = \frac{1}{2N}\sum_{i=1}^{N}(x_{i,1} + x_{i,2}) \tag{C.8}$$

and

$$s^2 = \frac{1}{2N}(\sum_{i=1}^{N}(x_{i,1} - \bar{x})^2 + \sum_{i=1}^{N}(x_{i,2} - \bar{x})^2) \tag{C.9}$$

.

Appendix D

PCB MEMS Accelerometer Calibration

MEMS accelerometers are typically factory calibrated, avoiding the user to perform any further calibration for the majority of the available applications. However, to reach a heading accuracy of bellow 2°, a simple calibration procedure [63] can be made and is hereafter described.

The relationship between the normalized accelerometer data a_x, a_y, and a_z and the raw accelerometer measurements A_{rx}, A_{ry}, and A_{rz} can be expressed as:

$$\begin{bmatrix} a_x \\ a_y \\ a_z \end{bmatrix} = \begin{bmatrix} ACC_{11} & ACC_{12} & ACC_{13} \\ ACC_{21} & ACC_{22} & ACC_{23} \\ ACC_{31} & ACC_{32} & ACC_{33} \end{bmatrix} \cdot \begin{bmatrix} A_{rx} \\ A_{ry} \\ A_{rz} \end{bmatrix} + \begin{bmatrix} ACC_{10} \\ ACC_{20} \\ ACC_{30} \end{bmatrix}. \tag{D.1}$$

The normalized values can be obtained for any given raw measurements after computing the 12 parameters from ACC_{10} to ACC_{33}. The calibration is performed by placing the sensor in 6 stationary positions, in all orthogonal directions, and collecting accelerometer raw data at each position during a time interval of 5 to 10 seconds.

Equation D.1 can be rewritten as:

$$\begin{bmatrix} a_x \\ a_y \\ a_z \end{bmatrix} = \begin{bmatrix} A_{rx} & A_{ry} & A_{rz} & 1 \end{bmatrix} \cdot \begin{bmatrix} ACC_{11} & ACC_{12} & ACC_{13} \\ ACC_{21} & ACC_{22} & ACC_{23} \\ ACC_{31} & ACC_{32} & ACC_{33} \\ ACC_{10} & ACC_{20} & ACC_{30} \end{bmatrix}. \tag{D.2}$$

Labeling the above matrices:

$$Y_a = W_a . X_a \tag{D.3}$$

- Y_a: known normalized earth gravity vector;
- W_a: sensor raw data collected at 6 stationary positions;
- X_a: calibration parameter matrix that needs to be determined.

Considering the ideal values for the 6 stationary positions, the following system is obtained:

$$\begin{bmatrix} 0 & 0 & 1 \\ 0 & 0 & -1 \\ 0 & 1 & 0 \\ 0 & -1 & 0 \\ 1 & 0 & 0 \\ -1 & 0 & 0 \end{bmatrix} = \begin{bmatrix} A_{rx1} & A_{ry1} & A_{rz1} & 1 \\ A_{rx2} & A_{ry2} & A_{rz2} & 1 \\ A_{rx3} & A_{ry3} & A_{rz3} & 1 \\ A_{rx4} & A_{ry4} & A_{rz4} & 1 \\ A_{rx5} & A_{ry5} & A_{rz5} & 1 \\ A_{rx6} & A_{ry6} & A_{rz6} & 1 \end{bmatrix} . \begin{bmatrix} ACC_{11} & ACC_{12} & ACC_{13} \\ ACC_{21} & ACC_{22} & ACC_{23} \\ ACC_{31} & ACC_{32} & ACC_{33} \\ ACC_{10} & ACC_{20} & ACC_{30} \end{bmatrix}, \tag{D.4}$$

where A_{rxn}, A_{ryn}, and A_{rzn} are the readings of the 6 stationary positions, with n samples. The calibration parameter matrix X_a can be determined by the least square method:

$$X_a = [{W_a}^T.W_a]^{-1}.{W_a}^T.Y. \tag{D.5}$$

Appendix E

Practical and experimental procedure

E.1 Experimental protocol

E.1.1 Security norms[1]

The entrance to the test room (ISR Shared Experimental Area) implies the mandatory use of a social mask and the consequent disinfection of the hands with alcohol gel. During the execution of the experiments, the windows must be open and all subjects must be present inside the room, with a maximum of 3. They must remain with the social mask, except for the participant during the exercise. Once the experiment is over, he must put on the social mask again. Any equipment used during the experiment must be properly disinfected before and after use. Between different acquisition periods, the windows must remain open and the fan turned on for a minimum period of 30 minutes.

E.1.2 Setup

- Xsens MVN inertial motion capture suite;
- *BodyEnergyExpenditure* prototype (includes a Polar H7 heart rate monitor, a Humon Hex muscle oximeter, and a *BITalino* (*r*)*evolution Plugged Kit BT*).

E.1.3 Schedule

Start of the sessions: July 17^{th} 2020.

End of the sessions: July 29^{th} 2020.

[1]Please take note that the experiments took place during the Covid-19 pandemic.

E.1.4 Participants

Parameters	Athletes (n=13)	Non-athletes (n=7)	All (n=20)
Female/Male	2/11	1/6	3/17
Age (years)	18.5 ± 3.0	26.6 ± 4.9	21.3 ± 5.4
Weight (kg)	67.8 ± 8.2	75.5 ± 14.4	70.5 ± 8.0
Height (m)	1.73 ± 0.06	1.74 ± 0.08	1.74 ± 0.06

Table E.1: Participant's characteristics.

E.1.5 Acquisition protocol

Procedures that precede the experiment

- Instructions about the experimental procedure;
- Questionnaire completion;
- Signature of the informed consent where the participant declares that he/she does not suffer from a disease that makes it impossible to participate in the tests and agrees with the collection of bio-metric and physiological data;
- Placement of the HR chest strap and heart rate calibration;
- Participant's instrumentation;
- Review of the experimental procedure.

Estimated time: 30-35min.

Experimental procedure

- MVN Suite calibration;
- Warm-up:
  - **Athlete**: 2 minutes at 4km/h, 2 minutes at 6.5km/h, 1 at minute 8km/h;
  - **Non-athlete**: 4 minutes at 4km/h, 1 minute at 6.5km/h;
- 12 minute test:
  - **Athlete**

- 3 minutes at 8km/h;
- 3 minutes at 9km/h;
- 6 minutes at 10km/h;
- **Non-athlete**
- 3 minutes at 6.5km/h;
- 3 minutes at 7.5km/h;
- 6 minutes at 8.5km/h;

- Recovery: 3 minutes at 4km/h.

Estimated time: 30-35min.

Procedures that follow the experiment

- Removal of the devices.

  Estimated time: 8-10min.

Equipment disinfection and space ventilation

Estimated time: 25-30min.

E.1.6 Timetable

Hours	July 20th	July 21th	July 22th	July 23th	July 24th	July 27th	July 28th	July 29th
09h00-10h30	AQUISITION	AQUISITION	AQUISITION	AQUISITION	AQUISITION	AQUISITION	AQUISITION	AQUISITION
10h30-11h00	D&V	D&V	D&V	D&V	D&V	D&V	D&V	D&V
11h00-12h30	AQUISITION	AQUISITION	AQUISITION	AQUISITION	AQUISITION	AQUISITION	AQUISITION	AQUISITION
12h30-13h00	D&V	D&V	D&V	D&V	D&V	D&V	D&V	D&V
13h00-15h00	----------	----------	----------	----------	----------	----------	----------	----------
15h00-16h30	AQUISITION	AQUISITION	AQUISITION	AQUISITION	AQUISITION	AQUISITION	AQUISITION	AQUISITION
16h30-17h00	D&V	D&V	D&V	D&V	D&V	D&V	D&V	D&V
17h00-18h30	AQUISITION	AQUISITION	AQUISITION	AQUISITION	AQUISITION	AQUISITION	AQUISITION	AQUISITION
18h30-19h00	D&V	D&V	D&V	D&V	D&V	D&V	D&V	D&V

Figure E.1: Timetable.

E.2 Authorization and informed consent

The current study aims to develop a prototype for estimating energy expenditure associated with physical exercise. For validation purposes, collections of physiological signals will be made at rest and during a 15-minute run. During the execution of the activity, several variables will be monitored, such as heart rate, accelerations of different parts of the body, muscle oxygenation and galvanic skin response. The data will be collected using a prototype made up of several sensors that will be distributed into different parts of the body. Throughout the experiment, images of the participant will also be collected, which will be kept anonymous, being only used for academic purposes. Before starting the experiment, a small questionnaire will be filled out regarding the individual's personal information (age, gender, height and weight), eating habits and other consumption, clinical history and participant's physical activity level. The time for data collection, plus the time required to complete the questionnaire, instrumentation of the participant and collection of the devices, will have a duration of approximately 1h30min. Participation is voluntary and the participant has the right to refuse to participate, or to give up at any time.

I, _____, *accept / allow my student to* (scratch as appropriate) participate in this study of data collection for the elaboration of a prototype meter of energy expenditure associated to physical exercise. I declare, for due legal purposes, that I authorize the capture of physiological signals during physical activity in laboratory environment, at the Systems and Robotics Institute of the University of Coimbra. I further expressly state that the said signals may be used in the context of scientific articles, books, dissertations or other types of material of scientific nature, and only in that context, renouncing any rights or possible compensation that could result from their use. I also declare that I authorize the anonymous disclosure of the signals collected in a database that will be exposed to the public.

E.3 Questionnaire

This questionnaire is part of a master's thesis in Electrical and Computer Engineering that aims to develop a prototype for estimating energy expenditure associated to physical exercise. All data collected in this questionnaire is anonymous and will only be used for academic purposes.

E.3.1 Personal data

Gender: Male ☐ Female ☐

Age: _____

Height: _____cm

Weight: _____kg

Nationality: _____

E.3.2 Eating habits and other consumption

What was your last meal?

Breakfast ☐ Lunch ☐ Snack ☐ Dinner ☐ Other: _____

Describe your last meal: _____

_____

How many meals you eat regularly per day? _____

Do you drink alcohol regularly? Yes ☐ No ☐

If yes, how often? _____

Have you consumed alcoholic beverages in the last 24 hours? Yes ☐ No ☐

Do you consume dietary supplements (vitamins, protein)? Yes ☐ No ☐

Do you smoke? Yes ☐ No ☐

E.3.3 Clinical history

Do you have history / suffer from any respiratory disease (asthma, pneumonia, rhinitis)?

Yes ☐ No ☐

Do you have any family members with history or who suffer from respiratory diseases?

Yes ☐ No ☐

Do you have history / suffer from any cardiovascular diseases (AVC, arrhythmia)?

Yes ☐ No ☐

Do you have any family members with history or who suffer from cardiovascular diseases?

Yes ☐ No ☐

Do you have history / suffer from any other chronic diseases?

Yes ☐ No ☐

Do you have any family members with history or who suffer from any other chronic diseases?

Yes ☐ No ☐

E.3.4 Fitness level

How often do you practice physical exercise? Select the best option for your case.

- ☐ Never
- ☐ Rarely
- ☐ 1x per week
- ☐ 2x per week
- ☐ 3x per week
- ☐ 4x per week or more

Do you currently practice any federated sport? Yes ☐ No ☐

If yes, which one? _____

How many practices per week? _____